

# **Gravitational Geons on the Brane**

by

Daniel John Kermode

B. Math, University of Waterloo, 1989

A THESIS SUBMITTED IN PARTIAL FULFILLMENT  
OF THE REQUIREMENTS FOR THE DEGREE OF

**MASTER OF SCIENCE**

in

THE COLLEGE OF GRADUATE STUDIES  
(Interdisciplinary Graduate Studies)

THE UNIVERSITY OF BRITISH COLUMBIA  
(Okanagan)

April 2011

© Daniel John Kermode, 2011

# Abstract

Gravitational geons, if they exist, represent a candidate for cosmological dark matter observations. Gravitational Geons that are nonsingular, asymptotically flat, topologically trivial spacetime solutions are not possible in General Relativity. The purpose of this thesis is to investigate whether such geons are possible on a 3 dimensional brane embedded in a 4+1 dimensional spacetime. Our approach is to identify the characteristics of a candidate spacetime solution on the brane, choose an example spacetime that exhibits those characteristics and determine if it corresponds to a gravitational geon.

# Preface

The original idea to investigate gravitational geons in brane-world cosmologies is that of my supervisor Dan Vollick. Together, we collaborated to author an article entitled *Gravitational Geons on the Brane* which has been submitted for publication at the journal *General Relativity and Gravitation*. Chapter 2 of this thesis is a version of that article.

The investigative effort involved in the article required extensive use of both analytical and numerical methods. Although we both participated in each effort, Professor Vollick's contributions were largely analytical whereas mine were largely numerical.

The writing of the article including the sourcing and verification of references was done by myself with extensive advice and support by Professor Vollick.

# Table of Contents

- Abstract . . . . . ii**
- Preface . . . . . iii**
- Table of Contents . . . . . iv**
- List of Figures . . . . . vi**
- List of Symbols . . . . . viii**
- Acknowledgments . . . . . x**
  
- 1 Introduction . . . . . 1**
  - 1.1 Differential Geometry and General Relativity . . . . . 2
    - 1.1.1 The Einstein Field Equations . . . . . 2
    - 1.1.2 The Kretschmann Scalar . . . . . 4
    - 1.1.3 Junction Conditions . . . . . 4
  - 1.2 The Brane-World . . . . . 6
  - 1.3 Gravitational Geons . . . . . 12
  - 1.4 Static Space-Time Solutions on the Brane . . . . . 16
    - 1.4.1 Brane-World Black Holes . . . . . 16
    - 1.4.2 Brane-World Wormholes . . . . . 19
  - 1.5 Gravitational Geons in Other Theories . . . . . 20
  
- 2 Gravitational Geons in Brane-World Cosmologies . . . . . 23**
  - 2.1 The Candidate Space-Times . . . . . 24
  - 2.2 Methods Of Investigation . . . . . 25

|          |  |           |
|----------|--|-----------|
| 2.2.1    | The Weak Field Approximation . . . . .       | 25        |
| 2.2.2    | Numerical Iteration . . . . .                | 26        |
| 2.2.3    | Direction Field Plots . . . . .              | 27        |
| 2.2.4    | Potential Singular Points . . . . .          | 28        |
| 2.3      | Weak Field Behaviour . . . . .               | 29        |
| 2.4      | General Behaviour . . . . .                  | 31        |
| 2.4.1    | Two Critical Points – High Range . . . . .   | 36        |
| 2.4.2    | Two Critical Points – Medium Range . . . . . | 37        |
| 2.4.3    | Two Critical Points – Low Range . . . . .    | 38        |
| 2.4.4    | No Critical Points . . . . .                 | 39        |
| <b>3</b> | <b>Discussion And Conclusion . . . . .</b>   | <b>43</b> |
| 3.1      | The Weak Field . . . . .                     | 43        |
| 3.2      | Identifying $m$ and $l$ . . . . .            | 44        |
| 3.3      | Suggestions for Further Analysis . . . . .   | 46        |
| 3.4      | Significance of the Result . . . . .         | 49        |
|          | <b>Bibliography . . . . .</b>                | <b>51</b> |

# List of Figures

|             |   |    |
|-------------|---|----|
| Figure 2.1  | The interface of a custom application built to investigate our candidate spacetimes using a fourth-order Runge-Kutta numerical iteration. . . . .   | 27 |
| Figure 2.2  | An example of a direction field plot showing numerical instabilities in $A(r)$ (here plotted for $l = 1$ , $m = 1.189$ and $1.25 < r < 1.42$ ). . . . .   | 28 |
| Figure 2.3  | $B(r)$ and $A(r)$ plotted against radius $r$ for $l = 1$ , $m = 0.01$ . A fourth-order numerical iteration of (2.5) is labelled $A(r)$ and the analytical weak field result is labelled <i>weak</i> $A(r)$ . These two approaches give almost identical results for $\frac{m}{l} \ll 1$ . . . . . | 30 |
| Figure 2.4  | $\alpha_1$ and $\beta_1$ plotted against $\frac{m}{l}$ for the first zero of $B'r + 4B$ . . . . .   | 33 |
| Figure 2.5  | $\alpha_1$ and $\beta_1$ plotted against $\frac{m}{l}$ for the second zero of $B'r + 4B$ . . . . .  | 33 |
| Figure 2.6  | $A(r)$ iteratively plotted against radius $r$ for $l = 1$ and $m = 1.25$ against a direction field plot. Here, both the convergence to $A = 0$ and $A = \frac{-\alpha_1}{\beta_1} \approx -1.84$ at the first zero of $B'r + 4B$ can be clearly seen. . . . .                                     | 36 |
| Figure 2.7  | Reverse iteration of $A(r)$ plotted against radius $r$ for $l = 1$ and $m = 1.192$ from the second zero of $B'r + 4B$ to the first, against a direction field plot. The solution is incompatible with the analytical result that $A' < 0$ at the first zero for $\lambda = 0$ solutions. . . . .  | 37 |
| Figure 2.8  | This direction field plot of $A(r)$ against radius $r$ shows that $A(r)$ is numerically unstable at the zeros of $B'r + 4B$ . Here we choose $l = 1$ and $m = 1.189$ such that the zeros are found at $r = 1.281, 1.392$ . . . . .  | 39 |
| Figure 2.9  | Forward iteration of $A(r)$ plotted from $r = 0$ to the first zero of $B'r + 4B$ for $l = 1$ and $m = 1.189$ . $A \rightarrow \frac{-\alpha_1}{\beta_1} \approx 1.38$ as the solution approaches the first zero. . . . .  | 40 |
| Figure 2.10 | Reverse iteration of $A(r)$ plotted from the second zero of $B'r + 4B$ to the first for $l = 1$ and $m = 1.189$ . . . . .   | 40 |

|             |   |    |
|-------------|---|----|
| Figure 2.11 | Forward iteration of $A(r)$ plotted from the second zero of $B'r + 4B$ for $l = 1$ and $m = 1.189$ . . . . .  | 41 |
| Figure 2.12 | The function $A(r)$ plotted against radius $r$ for $l = 1$ and $m = 1.189$ . A fourth-order Runge-Kutta numerical iteration was unable to navigate the zeros of $B'r + 4B$ (at $r = 1.281, 1.392$ ), so the result is constructed piecewise between these points. . . . . | 41 |
| Figure 2.13 | Function $A(r)$ plotted against radius $r$ . Here we choose $l = 1$ and chart a variety of values for $m$ in the specified region. A fourth-order Runge-Kutta numerical iteration is used to generate each result. . . . .  | 42 |
| Figure 3.1  | $B(r)$ plotted for $m = 1$ and $1 \leq l \leq 33.3$ . Note that all solutions have $\frac{m}{l} < \frac{32}{27}$ so these solutions all correspond to gravitational geons. . . . .  | 45 |

# List of Symbols

The following list contains primarily symbols whose physical and mathematical meaning remain unchanged throughout this thesis. Cited page numbers refer to the first occurrence of each symbol.

|                              |  |    |
|------------------------------|--|----|
| $R_{\mu\nu}, {}^{(5)}R_{AB}$ | Ricci tensor 4D/5D components (contracted from the Riemann tensor) . . . . .           | 2  |
| $R, {}^{(5)}R$               | Ricci scalar 4D/5D (contracted from the Ricci tensor) . . . . .                        | 2  |
| $T_{\mu\nu}, {}^{(5)}T_{AB}$ | energy momentum tensor 4D/5D components . . . . .                                      | 2  |
| $g_{\mu\nu}, {}^{(5)}g_{AB}$ | metric tensor 4D/5D components . . . . .   | 2  |
| $\Lambda, \Lambda_5$         | cosmological constant 4D/5D . . . . .  | 2  |
| $\kappa, \kappa_5$           | gravitational coupling constant 4D/5D . . . . .  | 2  |
| $B(r), B$                    | $g_{tt}$ metric tensor component of static, spherically symmetric space-time . . . . . | 3  |
| $A(r), A$                    | $g_{rr}$ metric tensor component of static, spherically symmetric space-time . . . . . | 3  |
| $O()$                        | <i>Order of</i> notation - terms of specified order and higher are neglected . . . . . | 4  |
| $S_{\mu\nu}, {}^{(5)}S_{AB}$ | surface energy momentum tensor 4D/5D components at a hypersurface . . . . .            | 5  |
| $K_{\mu\nu}, {}^{(5)}K_{AB}$ | extrinsic curvature tensor 4D/5D components . . . . .                                  | 5  |
| $\mathcal{L}_n$              | Lie differentiation operator . . . . .   | 6  |
| $R_{\mu\nu\sigma\phi}$       | The Riemann Curvature Tensor 4-dimensional components . . . . .                        | 9  |
| ${}^{(5)}R_{ABCD}$           | Riemann curvature tensor 5-dimensional components . . . . .                            | 9  |
| $\nabla_\mu$                 | covariant differentiation operator . . . . .   | 9  |
| ${}^{(5)}C_{ABCD}$           | Weyl curvature tensor 5-D components . . . . .   | 9  |
| $\mathcal{E}_{\mu\nu}$       | electric projection of the 5-D Weyl curvature tensor . . . . .                         | 10 |
| $\Gamma_{\mu\nu}^\alpha$     | Christoffel symbol for the Levi-Civita connection . . . . .                            | 14 |
| $\sqrt{-g}$                  | square-root of the determinant of the matrix of metric tensor components . . . . .     | 14 |
| $\partial_\alpha$            | partial derivative operator . . . . .  | 14 |
| $\eta_{\mu\nu}$              | Minkowski space-time metric tensor components . . . . .                                | 16 |



|                              |  |    |
|------------------------------|--|----|
| $b(r), b$                    | variation in $B(r)$ , defined in the weak field by $b(r) = 1 - B(r)$ ..... | 25 |
| $a(r), a$                    | variation in $A(r)$ , defined in the weak field by $a(r) = 1 - A(r)$ ..... | 25 |
| $\mathcal{B}_{\mu\nu\sigma}$ | magnetic projection of the 5-D Weyl curvature tensor .....                 | 47 |

# Acknowledgments

I would like to thank my supervisor, Professor Dan Vollick for his support and patience. It was Professor Vollick's original idea which led to the paper *Gravitational Geons on the Brane* which we collaborated to write and on which this thesis is based. I would also like to thank my wife Myra as well as my family and friends who have supported and encouraged me through my degree. I particularly appreciate the editorial review provided by Stephanie Halldorson.

For their excellent academic instruction and unqualified support, my gratitude goes to the professors of physics and mathematics at UBCO, in particular to Professor Erik Rosolowsky, Professor Murray Neuman and Professor Sylvie Desjardins.

This research was supported by the Natural Sciences and Engineering Research Council of Canada.

# Chapter 1

## Introduction

Einstein's general theory of relativity was published in 1915 and remains unsurpassed as a predictive mathematical model of gravitation. That having been said, general relativity also predicts the existence of space-time singularities in gravitational collapse (i.e. in black holes) and in cosmological space-times.

In particle physics, quantum field theory shares the predictive success of general relativity. In quantum field theory, one obstacle to unifying gravitation with the other forces of nature is the hierarchy problem which is related to the large discrepancy between the electro-weak scale and the Planck scale. The Randall-Sundrum *Brane-world* cosmological model [1] was proposed as a new way to solve the hierarchy problem. In this investigation, we consider Randall-Sundrum type brane-world cosmologies in which the three spatial dimensions of the observable universe are modeled by a 3 dimensional membrane or *3-brane* embedded in a 4+1 dimensional bulk space-time.

Long before brane-world theory was introduced, John Wheeler introduced the concept of a *gravitational-electromagnetic entity* or *geon* [2] with the hope that a configuration of gravitational and electromagnetic fields could form a persistent space-time *disturbance* that would ultimately provide a self-consistent picture of what a particle of matter is. A *gravitational geon* is a non-singular configuration of the gravitational field, without horizons that persists for a long period of time.

General relativity does not allow for static, topologically trivial and spherically symmetric gravitational geon solutions of the Einstein field equations. However,

in the Randall-Sundrum brane-world model, the 4+1 dimensional Einstein field equations in the bulk induce field equations on the brane that differ from those of general relativity.

In this thesis, we consider whether there are static, topologically trivial and spherically symmetric solutions to the Einstein field equations on the brane that correspond to gravitational geons. We construct these space-time solutions on the brane in order to prove that they could exist in Randall-Sundrum type brane-world cosmologies.

Our approach does not yield a general solution for gravitational geon space-times on the brane. However, using approximations and numerical methods, it does show that such space-time solutions exist.

Although the solutions that we find cannot correspond to conventional particles of matter, they could correspond to *dark matter*.

## 1.1 Differential Geometry and General Relativity

It is assumed that the reader is familiar with the mathematics of differential geometry and Einstein's general theory of relativity. In this thesis, we work extensively with the Einstein field equations and certain ideas specific to the study of curved manifolds. The intention of this section is to state and briefly review those results that form the foundation of this thesis. For further details, see [3–5].

We adopt the convention that the gravitational constant  $G$  and the speed of light  $c$  are dimensionally adjusted to unity.

### 1.1.1 The Einstein Field Equations

In general relativity, the Einstein field equations are

$$R_{\mu\nu} - \frac{1}{2}g_{\mu\nu}R = -g_{\mu\nu}\Lambda + \kappa T_{\mu\nu}, \quad (1.1)$$

where  $R_{\mu\nu}$  is the Ricci tensor (a contraction of the Riemann curvature tensor),  $R$  is the Ricci scalar (a contraction of the Ricci tensor),  $g_{\mu\nu}$  is the space-time metric,  $\Lambda$  is the cosmological constant,  $\kappa = 8\pi$  is the gravitational coupling constant and  $T_{\mu\nu}$  is the energy-momentum tensor representing the source of the gravitational field.

The left hand side of (1.1) describes the curvature of space whereas, ignoring the cosmological constant for the moment, the right hand side describes the distribution of matter and energy. In Misner, Thorne and Wheeler, [3], this interaction is described as "Space tells matter how to move" and "Matter tells space how to curve". Einstein added the cosmological constant to this equation to account for the general belief at the time that the universe is static on a cosmological scale.

The space-time metric is of the form

$$ds^2 = g_{\mu\nu}dx^\mu dx^\nu. \quad (1.2)$$

The metric for a static, spherically symmetric space-time solution can be written in the form (adopting the - + + + signature convention for this thesis)

$$ds^2 = -B(r)dt^2 + A(r)dr^2 + r^2(d\theta^2 + \sin^2\theta d\phi^2), \quad (1.3)$$

and the Ricci scalar is given by

$$R = \frac{B''}{AB} - \frac{B'}{2AB} \left( \frac{A'}{A} + \frac{B'}{B} \right) + \frac{2}{Ar} \left( \frac{B'}{B} - \frac{A'}{A} \right) + \frac{2}{Ar^2} - \frac{2}{r^2}. \quad (1.4)$$

In general relativity, for space-time solutions on scales much smaller than the cosmos (i.e. stars and galaxies), it is reasonable to take  $\Lambda = 0$  in 1.1. Vacuum solutions have  $T_{\mu\nu} = 0$  so that the Einstein field equations of general relativity reduce to

$$R_{\mu\nu} = 0 \quad (1.5)$$

In this thesis, we are investigating vacuum solutions on the brane. Insofar as the gravitational field equations on the brane are induced from the Einstein field equations in an embedding higher dimensional space-time, the field equations on the brane do not reduce to (1.5) in general.

We will see that there is a correspondence between vacuum solutions on the brane and solutions to the Einstein field equations in 3+1 dimensional general relativity with a trace-free energy-momentum tensor (i.e. with  $R = 0$  in the absence of a cosmological constant).

### 1.1.2 The Kretschmann Scalar

In our investigations, we be test candidate gravitational geon space-times. In particular, we are interested in static, spherically symmetric space-times that are non-trivial, non-singular and without horizons. For space-time metrics of the form (1.3), the Kretschmann scalar is derived from the Riemann curvature tensor as

$$R_{\mu\nu\rho\sigma}R^{\mu\nu\rho\sigma} = 4K_1^2 + 8K_2^2 + 8K_3^2 + 4K_4^2 \quad (1.6)$$

where [6]

$$K_1 = \frac{1}{A} \left( \frac{B''}{2B} - \frac{(B')^2}{4B^2} - \frac{A'B'}{4AB} \right) \quad (1.7)$$

$$K_2 = \frac{B'}{2ABr} \quad (1.8)$$

$$K_3 = \frac{-A'}{2A^2r} \quad (1.9)$$

$$K_4 = \frac{A-1}{Ar^2} \quad (1.10)$$

As this is a sum of squares of all components of the Riemann curvature tensor, a divergence in the Kretschmann scalar will correspond to a singularity in the space-time. It is clear from (1.9) and (1.10) that  $\lim_{r \rightarrow 0} A(r) = 1 + O(r^n)$  with  $n \geq 2$  to avoid divergence of the Kretschmann scalar. Similarly, from (1.8) it follows that  $\lim_{r \rightarrow 0} \frac{B'(r)}{B(r)} = O(r^m)$  with  $m \geq 1$ .

### 1.1.3 Junction Conditions

In the Randall-Sundrum model, the brane is a hypersurface embedded in a higher dimensional space-time. On the brane, we also encounter embedded hypersurfaces corresponding to potential singular points in the numerical analysis of our candidate brane-world space-times. In each situation involving an embedded hypersurface, the Israel-Darmois junction conditions must be met across the hypersurface.

Taking  $y$  to be a Gaussian normal coordinate orthogonal to the hypersurface (and letting  $y = 0$  at the hypersurface without loss of generality), the first junction condition is simply that there be no discontinuity in the metric

$$\lim_{y \rightarrow 0^+} g_{\mu\nu} - \lim_{y \rightarrow 0^-} g_{\mu\nu} = 0 \quad (1.11)$$

To get the second, we first observe that, in the embedding space-time around a hypersurface, the energy momentum tensor can be decomposed [7] as

$$T_{\mu\nu} = \theta(l)T_{\mu\nu}^+ + \theta(-l)T_{\mu\nu}^- + \delta(l)S_{\mu\nu} \quad (1.12)$$

where  $\theta(l)$  is the Heaviside theta function,  $\delta(l)$  is the Dirac delta function (both evaluated at the proper distance  $l$  from the hypersurface),  $T_{\mu\nu}^\pm$  is the energy-momentum tensor evaluated on either side of the hypersurface and  $S_{\mu\nu}$  is the surface energy-momentum tensor corresponding to the hypersurface.

The second Israel-Darmois junction condition states that the surface energy-momentum tensor corresponding to a hypersurface is related to the discontinuity in the extrinsic curvature  $K_{\mu\nu}$  across the hypersurface by [3, 8]

$$S_{\mu\nu} = \frac{1}{8\pi} ([K_{\mu\nu}] - [K]h_{\mu\nu}) \quad (1.13)$$

where  $h_{\mu\nu}$  is the induced metric on the hypersurface,  $K = K_\mu^\mu$  and the square brackets, indicate the discontinuity in a physical quantity crossing the hypersurface (i.e.  $[K] = K^+ - K^-$ ).

In the Randall-Sundrum brane-world cosmology, we will look at solutions to the gravitational field equations on the brane embedded in a higher dimensional bulk space-time. The solution on the hypersurface is known, but the solution in the embedding space-time is not. The effective Einstein field equations on the brane include terms involving  $S_{\mu\nu}$ . (1.13) is used to show that these terms are zero for static, vacuum space-time solutions on the brane.

We will also examine solutions to the 3+1 dimensional Einstein field equations that can only be constructed piece-wise around embedded hypersurfaces where we find numerical instabilities. The solution on the hypersurface is unknown but the solution in the embedding space-time is. In this situation, the extrinsic curvature

can be evaluated using [4]

$$K_{\mu\nu} = \frac{1}{2}\mathcal{L}_n g_{\mu\nu} \quad (1.14)$$

where  $\mathcal{L}_n$  is the Lie Derivative with respect to the normal of the hypersurface in question. The extrinsic curvature is evaluated in the limit approaching the hypersurface from either side. Should there be a discontinuity in  $K_{\mu\nu}$  across the hypersurface,  $S_{\mu\nu} \neq 0$  in general. This is generally taken to mean that there is a gravitational source (other than the gravitational field) present at the hypersurface. In this thesis, we are interested in vacuum solutions and so require that gravitational solutions have continuity of the extrinsic curvature across every such hypersurface.

## 1.2 The Brane-World

Einstein's theory of general relativity is a 4 dimensional theory, the dimensions being the 3 spatial dimensions of our universe and time. Space-time models that incorporate more than 4 dimensions date back to the theory of Kaluza who showed that 5 dimensional general relativity could incorporate both the 4 dimensions of Einstein's gravitational theory and Maxwell's theory of electromagnetism [9]. As we only experience a 3+1 dimensional space-time, Kaluza made the assumption that the metric would not change with respect to the extra dimension. In effect, physics would take place on a 4 dimensional hypersurface in a 5 dimensional space-time [11]. Klein showed that this condition would arise naturally if the 5th dimension had a circular topology on a small enough scale [10]. That being the case, the energies of all modes above the ground state of a Fourier expansion of the periodic dependence of any physical field on the 5th dimension, could be made so high as to be unobservable.

The success of this unification of gravitation and electromagnetism led physicists to theories with higher dimensions with the hope of unifying gravitation and electromagnetism with the strong and weak forces. 10 dimensional string theories and eventually the 11 dimensional M-theory emerged from these efforts. In string theory, the 6 extra dimensions are compact and small as is the extra dimension in the Kaluza-Klein theory. M-theory extends 10-dimensional string theory with one



extra dimension the size of which depends on the string coupling strength.

M-theory introduced the idea that there could be an extra dimension whose scale is large relative to the fundamental scale. This idea forms the basis of Randall-Sundrum models of 5-dimensional gravity in which the three spatial dimensions of the empirical universe are a 3 dimensional membrane or *3-brane* embedded in a 4+1 dimensional space-time (*4+1 dimensional* referring to four spatial dimensions and time). Particles and forces of the standard model are confined to the brane whereas the gravitational field can propagate through the bulk.

The Randall-Sundrum models were proposed as a new mechanism for solving the hierarchy problem. The hierarchy problem is related to the fact that the fundamental energy scale at which the quantum effects of gravity become strong (known as the Planck scale) is so much larger than the energy scale at which the quantum effects of the other forces become strong. In the Randall-Sundrum model, gravitation is free to propagate through the bulk whereas the other forces are confined to the brane. The fundamental energy scale in the bulk can therefore be much smaller than the Planck scale, which remains the effective fundamental energy scale on the brane.

It is the Randall and Sundrum [1, 12] single brane model which provides the mathematical framework for our investigations. The effective 3+1 dimensional Einstein field equations on the brane were derived by Shiromizu, Maeda, and Sasaki [13]. An excellent review of this work is provided by [14] (see also [15–20]).

The Einstein field equations in the 4+1 dimensional bulk space-time are

$${}^{(5)}R_{AB} - \frac{1}{2}{}^{(5)}g_{AB}{}^{(5)}R = -{}^{(5)}g_{AB}\Lambda_5 + \kappa_5^2{}^{(5)}T_{AB} \quad (1.15)$$

where the terms are the same as for the 3+1 dimensional case (1.1) except <sup>(5)</sup> preceding a tensor or <sub>5</sub> following a scalar indicates the appropriate dimensionality (the convention that upper case latin indices indicate bulk tensors with lower case greek indices indicating 3+1 dimensional tensors on the brane is also used).

The metric in the bulk will be

$${}^{(5)}ds^2 = {}^{(5)}g_{AB}dx^A dx^B \quad (1.16)$$

If we let  $y$  be a Gaussian normal coordinate orthogonal to the brane (letting  $y = 0$  at the brane without loss of generality) then

$${}^{(5)}ds^2 = {}^{(4)}g_{\mu\nu}(x^\alpha, y)dx^\mu dx^\nu + dy^2 \quad (1.17)$$

where  ${}^{(4)}g_{\mu\nu}(x^\alpha, y)$  corresponds to induced metric on the hypersurfaces at  $y = \text{constant}$ . The 3+1 dimensional metric on the brane is therefore  ${}^{(4)}g_{\mu\nu}(x^\alpha, 0)$  (which we will generally write as  $g_{\mu\nu}$ ).

Our objective in this section is to determine the induced Einstein field equations on the brane. We begin by taking the string theory idea that the fields of the standard model (i.e. electromagnetic, strong, weak and all matter) are confined to the brane. Gravitation is the only field that is permitted to extend into the bulk. Thus if  $T_{\mu\nu}$  is the 4 dimensional energy-momentum tensor of the particles and fields confined to the brane then the total energy momentum tensor on the brane is

$$T_{\mu\nu}^{brane} = T_{\mu\nu} - \lambda g_{\mu\nu} \quad (1.18)$$

where  $\lambda$  is the *brane tension* which tends to prevent the gravitational field from *leaking* into the bulk. Insofar as this model represents a departure from standard general relativity, the accuracy to which general relativity predicts gravitation in experiment puts a lower limit on the brane tension of  $\lambda > (1 \text{ TeV})^4$ .

In (1.17), the use of a 4-dimensional tensor in a 5-dimensional equation is fairly explicit by nature of the coordinate system used. However, we wish to decompose the the 5-dimensional energy-momentum tensor into a part that resides on the brane and those parts that do not. This requires that we include the tensor  $T_{\mu\nu}^{brane}$ , which is 4-dimensional in a 5-dimensional equation. We do this by defining the 4-dimensional tensor in terms of a 5-dimensional tensor as

$$\begin{aligned} T_{\mu\nu}^{brane} &= {}^{(5)}T_{AB}^{brane} g_\mu^A g_\nu^B, \\ {}^{(5)}T_{AB}^{brane} n^A &= {}^{(5)}T_{AB}^{brane} n^B = 0 \end{aligned} \quad (1.19)$$

where  $n^B$  is normal to the brane. The behaviour of  ${}^{(5)}T_{AB}^{brane}$  off the brane is not important insofar as we decompose the bulk energy-momentum as

$${}^{(5)}T_{AB} = {}^{(5)}\tilde{T}_{AB} + T_{AB}^{brane} \delta(y) \quad (1.20)$$

where the delta function expresses the confinement of standard model particles and fields to the brane at  $y = 0$ . We can now rewrite (1.15) incorporating this to give

$${}^{(5)}R_{AB} - \frac{1}{2}{}^{(5)}g_{AB}{}^{(5)}R = -{}^{(5)}g_{AB}\Lambda_5 + \kappa_5^2 \left( {}^{(5)}\tilde{T}_{AB} + T_{AB}^{brane} \delta(y) \right) \quad (1.21)$$

In order to determine the induced Einstein field equations on the brane, in addition to the induced energy-momentum tensor, we need to know the induced Riemann curvature tensor on the brane. The bulk Riemann curvature tensor is projected onto 4 dimensional hypersurfaces  $y = \text{const.}$  (with extrinsic curvature corrections) as

$$R_{\mu\nu\sigma\rho} = {}^{(5)}R_{ABCD}g_{\mu}{}^A g_{\nu}{}^B g_{\sigma}{}^C g_{\rho}{}^D + 2K_{\mu[\sigma}K_{\rho]\nu} \quad (1.22)$$

in which the square brackets denote anti-symmetrization. The change in the extrinsic curvature  $K_{\mu\nu}$  along the  $y = \text{const.}$  surfaces is projected from the bulk Ricci tensor via the Codazzi equation

$$\nabla_{\nu}K^{\nu}{}_{\mu} - \nabla_{\mu}K = {}^{(5)}R_{AB}g_{\mu}{}^A n^B, \quad (1.23)$$

where  $K = K^{\nu}{}_{\nu}$ .

Observing that the 5-dimensional Riemann curvature tensor can be written as

$${}^{(5)}R_{ABCD} = {}^{(5)}C_{ACBD} + \frac{2}{3} \left( {}^{(5)}g_{A[C}{}^{(5)}R_{D]B} - {}^{(5)}g_{B[C}{}^{(5)}R_{D]A} \right) - \frac{1}{6}{}^{(5)}g_{A[C}{}^{(5)}g_{D]B}{}^{(5)}R, \quad (1.24)$$

where  ${}^{(5)}C_{ACBD}$  is the Weyl tensor (which is trace free). Further observing that  ${}^{(5)}\tilde{T}_{AB} = 0$  (i.e. there are no stresses other than the cosmological constant and those on the brane) then combining (1.21) and (1.22) gives an expression for the induced Einstein field equations on the brane

$$\begin{aligned}
R_{\mu\nu} - \frac{1}{2}g_{\mu\nu}R &= -\frac{1}{2}\Lambda_5 g_{\mu\nu} + \frac{2}{3} \left( T_{\mu\nu}^{brane} - \frac{1}{4}T^{brane} g_{\mu\nu} \right) + KK_{\mu\nu} \\
&- K_{\mu}^{\alpha} K_{\alpha\nu} + \frac{1}{2}(K^{\alpha\beta} K_{\alpha\beta} - K^2)g_{\mu\nu} - \mathcal{E}_{\mu\nu}, \tag{1.25}
\end{aligned}$$

where

$$\mathcal{E}_{\mu\nu} = {}^{(5)}C_{ACBD} n^C n^D g_{\mu}^A g_{\nu}^B \tag{1.26}$$

is the *electric* projection of the 5 dimensional Weyl tensor and, by virtue of Weyl tensor symmetries, is trace-free.

Now, Randall-Sundrum brane-world cosmologies are  $Z_2$ -symmetric (have mirror symmetry) so that the bulk space-time looks the same approaching the brane from one side as it does emerging from it on the other, but with the normal reversed. Consequently, we can say that the extrinsic curvature in the limit as  $y \rightarrow 0$  approaching the brane from either side satisfies

$$\lim_{y \rightarrow 0^+} K_{AB} = - \lim_{y \rightarrow 0^-} K_{AB} \tag{1.27}$$

The Israel Darmois junction conditions for a 4+1 dimensional bulk space-time are derived by integrating (1.21) across the brane taking the limit from either side giving

$$\lim_{y \rightarrow 0^+} g_{AB} - \lim_{y \rightarrow 0^-} g_{AB} = 0, \tag{1.28}$$

$$\lim_{y \rightarrow 0^+} K_{AB} - \lim_{y \rightarrow 0^-} K_{AB} = -\kappa_5^2 \left( {}^{(5)}T_{AB}^{brane} + \frac{1}{3}T^{brane} g_{AB} \right), \tag{1.29}$$

which, applying (1.27) and (1.18) gives the extrinsic curvature on the brane

$$K_{\mu\nu} = -\frac{1}{2}\kappa_5^2 \left( T_{\mu\nu} + \frac{1}{3}(\lambda - T)g_{\mu\nu} \right), \tag{1.30}$$

So we can write the contributions from the extrinsic curvature in (1.25) in terms of the energy momentum tensor. This contribution is written

$$S_{\mu\nu} = \frac{1}{12}TT_{\mu\nu} - \frac{1}{4}T_{\mu\alpha}T^{\alpha}_{\nu} + \frac{1}{24}g_{\mu\nu}\left(3T_{\alpha\beta}T^{\alpha\beta} - T^2\right). \quad (1.31)$$

where, recalling 1.18,  $T_{\mu\nu}$  is the 4-dimensional energy-momentum tensor of the particles and fields confined to the brane.

If there are any stresses in the bulk other than the bulk cosmological constant (i.e. if  ${}^{(5)}\tilde{T}_{AB} \neq 0$ ), they will also affect the induced Einstein field equations on the brane. In our case we assume there are none so the induced Einstein field equations on the brane become

$$R_{\mu\nu} - \frac{1}{2}g_{\mu\nu}R = -g_{\mu\nu}\Lambda + \kappa^2 T_{\mu\nu} + 6\frac{\kappa^2}{\lambda}S_{\mu\nu} - \mathcal{E}_{\mu\nu}, \quad (1.32)$$

where  $\kappa^2$  is an effective coupling constant inherited from the fundamental coupling constant and the cosmological constant on the brane

$$\Lambda = \frac{1}{2}(\Lambda_5 + \kappa^2\lambda), \quad (1.33)$$

will be zero as we assume that the bulk cosmological constant will be balanced by the brane tension  $\lambda$ .

We will be working only with vacuum solutions on the brane (i.e.  $T_{\mu\nu} = 0$ ). As a consequence, equation (1.32) simplifies to

$$R_{\mu\nu} - \frac{1}{2}g_{\mu\nu}R = -\mathcal{E}_{\mu\nu}. \quad (1.34)$$

We know that  $\mathcal{E}_{\mu\nu}$  is trace free (i.e.  $\mathcal{E}_{\mu}^{\mu} = 0$ ) so contracting both sides of (1.34) yields

$$\begin{aligned} R_{\mu}^{\mu} &= \mathcal{E}_{\mu}^{\mu} = 0, \\ R_{\mu\nu} &= -\mathcal{E}_{\mu\nu}, \end{aligned} \quad (1.35)$$

and that, for vacuum solutions,

$$\nabla^{\mu}\mathcal{E}_{\mu\nu} = 0, \quad (1.36)$$

where  $\nabla_\mu$  is the covariant derivative on the brane.

In standard 3+1 dimensional general relativity (with no cosmological constant), the Einstein field equations for a solution to  $R = 0$  (so not a vacuum solution in general) will reduce to

$$R_{\mu\nu} = 8\pi T_{\mu\nu}, \quad (1.37)$$

with  $\nabla^\mu T_{\mu\nu} = 0$ . We therefore make the correspondence

$$8\pi T_{\mu\nu} = -\mathcal{E}_{\mu\nu}. \quad (1.38)$$

The result is that, as stated by Dadhich, Maartens, Papadopoulos and Reznia [21]

*A stationary general relativity solution with trace-free energy-momentum tensor gives rise to a vacuum brane-world solution in 5-dimensional gravity.*

The candidate gravitational geon space-time solutions that we will be investigating are stationary vacuum solutions on the brane. In standard general relativity, such solutions would have to satisfy  $R_{\mu\nu} = 0$ . However, in the brane-world cosmologies considered herein, we solve  $R = 0$  to obtain non-vacuum (in general), 3+1 dimensional space-time solutions to general relativity and these will correspond to 4+1 dimensional, vacuum solutions on the brane.

### 1.3 Gravitational Geons

In 1955, John Archibald Wheeler coined the term *geon* as an abbreviation for gravitational-electromagnetic entity [2]. He wrote the following description of a geon:

*Associated with an electromagnetic disturbance is a mass, the gravitational attraction of which under appropriate circumstances is capable of holding the disturbance together for a long time in comparison with the characteristic periods of the system.*

Wheeler's intention was to provide a self-consistent picture of what a body of matter is. More than half a century later, we still do not have a consensus on what

that picture should be.

In quantum field theory, particles of matter are considered to be field quanta but there is no accepted understanding of how the gravitational field should be quantized. General relativity provides an effective model of gravitation in terms of the geometry of space-time, but in its original form, general relativity does not explain what matter is or how the other forces of nature come about.

In the years immediately following the introduction of the geon, work focused on geons that included electromagnetic waves. Regge and Wheeler introduced the idea of gravitational geons in 1957 [22]. These were defined as geons that consisted only of gravitational waves.

In general relativity, the gravitational field corresponds to curvature in a 3+1 dimensional space-time. Solutions to the field equations of general relativity are considered topologically trivial if they are topologically equivalent to a Minkowski space-time (i.e. the solution can be obtained by continuously deforming a flat 3+1 dimensional space-time).

In general relativity (and Kaluza's 5 dimensional generalization [9]), there are no non-singular, topologically trivial solutions representing a gravitational field of non-vanishing mass [23, 24] (see also [25, 26] and [27] in particular for historical context).

Our investigations are concerned with static, topologically trivial, non-singular gravitational geon solutions for brane-world cosmologies. We know that such solutions are not possible in 3+1 dimensional general relativity, but in brane-world cosmologies, the induced Einstein field equations on the brane differ from those of general relativity. In particular, in brane-world cosmologies, vacuum solutions on the brane correspond to solutions to  $R = 0$  in general relativity whereas in vacuum solutions of general relativity require  $R_{\mu\nu} = 0$ .

It is useful to briefly consider why gravitational geon solutions cannot satisfy the condition that  $R_{\mu\nu} = 0$ . In his 1923 theorem, Birkhoff [28] showed that the Schwarzschild metric is the unique spherically symmetric vacuum solution in general relativity. As we are interested in non-singular, spherically symmetric vacuum solutions without horizons of the form (1.3), this result is sufficient for our purposes as the Schwarzschild metric has both a horizon and is singular at its radial origin. However, Einstein and Pauli [23, 24] did not impose spherical symmetry

and worked with Kaluza's 5 dimensional generalization of general relativity (which is a foundational concept for string theory and, consequently brane-world cosmologies). Their work is therefore more relevant to the study of gravitational geons in brane-world cosmologies than Birkhoff's theorem. For that reason, I present here a simplification to the spherically symmetric case, of Einstein and Pauli's work .

In 3+1 dimensional general relativity, Einstein and Pauli considered the variation of the Ricci tensor

$$\delta R_{\mu\nu} = -\nabla_\alpha(\delta\Gamma_{\mu\nu}^\alpha) + \nabla_\nu(\delta\Gamma_{\mu\alpha}^\alpha). \quad (1.39)$$

We can then define the vector density  $\mathfrak{K}^\alpha$  by

$$\partial_\alpha \mathfrak{K}^\alpha = \sqrt{-g} g^{\mu\nu} \delta R_{\mu\nu}, \quad (1.40)$$

so that

$$\mathfrak{K}^\alpha = \sqrt{-g}(g^{\mu\alpha} \delta\Gamma_{\mu\nu}^\nu - g^{\mu\nu} \delta\Gamma_{\mu\nu}^\alpha). \quad (1.41)$$

We are interested in vacuum solutions, so we only consider variations that preserve  $R_{\mu\nu} = 0$ . For any such variation, we have that  $\delta R_{\mu\nu} = 0$  and hence

$$\partial_\alpha \mathfrak{K}^\alpha = 0. \quad (1.42)$$

In the following treatment we consider only space-time solutions of the form (1.3) thus,  $g_{tt}$  and  $g_{rr}$  are both functions only of  $r$ . In our notation, we continue to use lower-case Greek indices ( $\alpha, \beta$ , etc.) to indicate tensors on a 3+1 dimensional space-time; we use specific lower-case latin letters ( $i, j, k$ ) to indicate tensors on 3 dimensional space and we use  $[t, r, \theta, \phi]$  as the indices of 3+1 dimensional space-time in spherical polar coordinates.

To avoid singularities (and for consistency with the candidate space-times that we examine in this thesis), we consider only solutions for which  $g_{tt}$  and  $g_{rr}$  are both non-zero and finite for all  $r \geq 0$ . The variation that we are considering can be written as a coordinate transformation

$$x^\alpha = x^\alpha + \xi^\alpha. \quad (1.43)$$



Retaining only terms of the first order in the infinitesimal variation  $\xi^\alpha$ , we have

$$\delta\Gamma_{\mu\nu}^\alpha = -\partial_\mu\partial_\nu\xi^\alpha + \partial_\sigma(\xi^\alpha)\Gamma_{\mu\nu}^\sigma - \partial_\mu(\xi^\sigma)\Gamma_{\sigma\nu}^\alpha - \partial_\nu(\xi^\sigma)\Gamma_{\sigma\mu}^\alpha - \xi^\sigma\partial_\sigma\Gamma_{\mu\nu}^\alpha. \quad (1.44)$$

We are interested in coordinate transformations that preserve the static nature of the space-time solutions. Einstein and Pauli [24] considered specific transformations that lead to an integral theorem that singles out the regular solutions of  $R_{\mu\nu} = 0$  and are defined by

$$\xi^t = c_1 t, \quad \xi^r = 0, \quad \xi^\theta = 0, \quad \xi^\phi = 0. \quad (1.45)$$

Substituting (1.44) into (1.41), (1.42) therefore becomes

$$\partial_i(\sqrt{-g}g^{tt}\Gamma_{tt}^i) = 0, \quad (1.46)$$

where  $i$  only sums over the 3 spatial dimensions since we are only considering static space-time solutions (i.e.  $\partial_t g_{\mu\nu} = 0$ ). This simplifies to

$$\partial_r(\sqrt{-g}g^{tt}g^{rr}\partial_r(g_{tt})) = 0. \quad (1.47)$$

Multiplying (1.47) through by  $g_{tt}$  gives

$$\partial_r(g_{tt})\sqrt{-g}g^{tt}g^{rr}\partial_r(g_{tt}) = \partial_r(g_{tt}\sqrt{-g}g^{tt}g^{rr}\partial_r(g_{tt})), \quad (1.48)$$

which integrating over a 3 dimensional, singularity-free region and applying Gauss' theorem gives

$$\int_V \sqrt{-g}g^{tt}g^{rr}(\partial_r(g_{tt}))^2 dV + \oint_S \sqrt{-g}g^{rr}\partial_r(g_{tt})n_r dS = 0. \quad (1.49)$$

As the surface  $S$  approaches infinity,  $g_{tt} \rightarrow -1$  and  $g^{rr} \rightarrow 1$  so that

$$\oint_S \sqrt{-g}g^{rr}\partial_r(g_{tt})n_r dS \rightarrow 0. \quad (1.50)$$

Therefore,

$$\int_V \sqrt{-g} g^{tt} g^{rr} (\partial_r(g_{tt}))^2 dV \rightarrow 0, \quad (1.51)$$

as the boundary of the volume  $V$  approaches infinity. As  $g^{tt} < 0$ ,  $\sqrt{-g} > 0$  and  $g^{rr} > 0$  for all  $r \geq 0$ , it must be the case that  $g_{tt} = \text{constant}$ . For vacuum solutions we therefore have  $R_{ij} = 0$ , but in three dimensions this implies that the space is Euclidean.

The requirement that  $R_{\mu\nu} = 0$  therefore implies that there can be no static, spherically symmetric, topologically trivial and non-singular space-time solutions (i.e. gravitational geons of the type we are investigating) in 3+1 dimensional general relativity.

However, in Randall-Sundrum brane-world cosmologies, vacuum space-time solutions must satisfy  $R = R_\alpha^\alpha = 0$  but not  $R_{\mu\nu} = 0$ . Thus, gravitational geon solutions of brane-world space-times may therefore be possible.

## 1.4 Static Space-Time Solutions on the Brane

This thesis explores the possibility that space-time solutions that correspond to gravitational geons may exist in brane-world cosmologies. Insofar as there has been considerable interest in brane-world cosmological models, there are recently published articles regarding other static space-time solutions on the brane that have some aspects in common with the investigations of this thesis. The following sections briefly summarize articles that investigate solutions corresponding to black holes and wormholes on the brane.

### 1.4.1 Brane-World Black Holes

There are a number of different ways that brane-world black holes have been considered. In 2000, Chamblin, Hawking and Reall [29] looked at the metric for a black string in a 4+1 dimensional anti de Sitter (AdS) space-time. They wrote the AdS space-time metric

$$ds^2 = e^{\frac{-2y}{l}} \eta_{\mu\nu} dx^\mu dx^\nu + dy^2, \quad (1.52)$$

where  $\eta_{\mu\nu}$  is the 4-dimensional Minkowski metric and  $l$  is the AdS radius. They

introduced the coordinate  $z = le^y$  so that the black string metric could be written as

$$ds^2 = \frac{l^2}{z^2} (-U(r)dt^2 + U(r)^{-1}dr^2 + r^2(d\theta^2 + \sin^2\theta d\phi^2) + dz^2), \quad (1.53)$$

where  $U(r) = 1 - \frac{2M}{r}$ . They then pointed out that this metric, with an appropriate rescaling of the coordinates  $r$  and  $t$ , is in standard Schwarzschild form on the brane (at  $y = 0$  hence  $z = l$ ). A black string in the bulk thus defined gives rise to a Schwarzschild black hole on the brane.

Later in the same year, Dadhich, Maartens, Papadopoulos and Rezania [21] considered the problem a different way. Instead of starting with a solution on the bulk space-time, they started (as do we) by insisting that their solution solve the induced Einstein field equations on the brane. They showed that a static, spherically symmetric black hole solution of the form (1.3) is given by

$$B(r) = A(r)^{-1} = 1 - \left(\frac{2M}{M_p^2}\right) \frac{1}{r} + \left(\frac{q}{\tilde{M}_p^2}\right) \frac{1}{r^2}, \quad (1.54)$$

where  $M_p$  is the Planck mass on the brane,  $\tilde{M}_p$  is the Planck mass in the bulk, and  $q$  is a dimensionless *tidal charge* parameter (so named because of its correspondence to the charge parameter in the Reissner-Nördstrom black hole in general relativity).

In general relativity, the charge parameter  $Q$  in the Reissner-Nördstrom black hole solution is squared and so always acts to weaken the gravitational field of the black hole (as compared to a Schwarzschild solution which is achieved in the limit as  $Q \rightarrow 0$ ). In their discussion of this brane-world black hole solution, the authors pointed out that the tidal charge parameter  $q$  is negative corresponding to a negative effective energy density on the brane contributed by the free gravitational field in the bulk. Consequently, the bulk effects tend to strengthen the gravitational field of the black hole as compared to a Schwarzschild black hole (achieved in the limit as  $q \rightarrow 0$ ).

In 2002, Vollick [19] showed that solving  $R = 0$  for space-time metrics of the form (1.3) with  $A(r) = B(r)^{-1}$  has the general solution

$$B(r) = A(r)^{-1} = 1 + \frac{\alpha}{r} + \frac{\beta}{r^2}, \quad (1.55)$$

where  $\alpha$  and  $\beta$  are constants. Thus the Reissner-Nördstrom type solution of Dadhich, Maartens, Papadopoulos and Rezania is the most general of that form. He then considered the result if the condition that  $A(r) = B(r)^{-1}$  is removed and  $B(r) = 1 - \frac{2m}{r}$  (i.e.  $g_{tt}$  is Schwarzschild). He obtained the solution

$$A(r) = \left(1 - \frac{2m}{r}\right)^{-1} \left[\frac{3m - 2r}{\lambda - 2r}\right]. \quad (1.56)$$

It was suggested that deviations from Schwarzschild geometry (which must result from the Weyl term in the induced Einstein field equations on the brane as in (1.26)) could be responsible for observations attributed to dark matter.

A third distinct approach to brane-world black holes is that of Shankaranarayanan and Dadhich in 2004 [30]. They considered the possibility of non-singular black holes on the brane. They obtained a non-singular Reissner-Nördstrom type black hole solution in a  $D$ -dimensional, spherically symmetric space-time (where  $D \geq 5$ ) with a metric of the form

$$ds^2 = -B(r)dt^2 + A(r)dr^2 + r^2d\Omega^2, \quad (1.57)$$

where  $d\Omega^2$  is the  $(D - 2)$ -dimensional angular line-element. The solution that they obtained had

$$B(r) = A(r)^{-1} = 1 - \frac{4R_g(r)}{(D - 2)r^{D-3}}, \quad (1.58)$$

where

$$R_g(r) = 4\pi \int_0^r \rho(x)x^{D-2}dx. \quad (1.59)$$

Having found the form of their solution, the authors proceeded to choose mass and charge distributions in order to set  $\rho(x)$  in (1.59). This led to them arriving (with some simplifying assumptions) at the expression

$$\begin{aligned}
B(r) = A(r)^{-1} = & 1 - \frac{16\pi}{(D-2)(D-1)} \frac{1}{r^{D-3}} \frac{c_1}{c_2} (1 - \exp(-c_2 r^{D-1})) \\
& + \frac{16\pi c_3}{(D-2)(D-3)} \frac{1}{r^{2(D-3)}} (1 - \exp(-c_4 r^{2(D-2)})) \quad (1.60)
\end{aligned}$$

where the  $c_i$ 's are constants.

The induced black hole solution on the brane is non-singular and admits one horizon. In order to achieve this result, they had to relax the condition that  $R = 0$ . In our investigation, we insist on a vanishing Ricci scalar in the induced Einstein field equations on the brane (1.34). In the brane-world black hole of Shankaranarayanan and Dadhich contributions to  $R$  cannot come from the bulk Weyl tensor via  $\mathcal{E}_{\mu\nu}$  as this tensor is trace-free. The non-vanishing Ricci scalar indicates a varying cosmological constant-like term, thus the gravitational geons that we investigate in this thesis differ fundamentally from their result.

#### 1.4.2 Brane-World Wormholes

As with black hole solutions on the brane, when investigating wormhole solutions on the brane there are two fundamental approaches. One can either create a wormhole solution in the bulk space-time and examine the induced solution on the brane (see for example [31]), or one can create a wormhole solution that satisfies the induced Einstein field equations on the brane.

In their 2002 paper, Bronnikov and Kim [6] take the latter approach. They begin with a generic, static, spherically symmetric space-time metric on the brane, as do we (1.3). Our method is comparable to theirs insofar as they also solve for  $R = 0$  and test for finiteness of the Kretschmann scalar (1.1.2) as a regularity criterion for the resulting space-time solutions.

The brane-world wormhole solutions considered were, like our gravitational geon solutions, static, spherically symmetric, non-singular and without horizons. However, for a wormhole, the solution need only be non-singular for  $r > r_0$  for some  $r_0 > 0$ . Two space-time solutions meeting this condition can be *sewn together* at the spherical hypersurface at  $r_0$  (which is identified as the *throat*). The resulting piece-wise constructed space-time forms the wormhole provided the Israel-

Darmois junction conditions (1.1.3) are met at the throat.

The authors considered both symmetric and asymmetric brane-world wormhole metrics. One example given of a symmetric wormhole solution used the metric [32]

$$ds^2 = -dt^2 + \left(1 - \frac{r_0}{r}\right)^{-1} dr^2 + r^2(d\theta^2 + \sin^2\theta d\phi^2). \quad (1.61)$$

It is clear that  $g_{rr} \rightarrow -\infty$  as  $r \rightarrow r_0$ . Bronnikov and Kim assert that the creation of wormholes involves the violation of the null energy condition at least in a neighbourhood of the throat. In brane-world cosmologies, a negative energy density that would provide for this violation is possible (see [33]). The surface energy-momentum tensor (1.12) associated with the throat of the wormhole may have contributions from the Weyl term in the induced field equations on the brane (1.26).

The authors do not attempt to evolve the brane-world metric into the bulk in order to discover what those contributions are for any particular solution.

## 1.5 Gravitational Geons in Other Theories

As we have seen, general relativity does not admit static, non-singular and topologically trivial gravitational geon solutions. As a consequence, most work on gravitational geons has considered concentrations of gravitational waves (see for example [34] and, for an argument that this type of solution is inadmissible as a gravitational geon in general relativity, [35, 36]) or *topological geons* (particles made from non-trivial spatial topology [37]).

This thesis investigates whether topologically trivial gravitational geons are possible in brane-world cosmologies based on the observation that the effective Einstein field equations on the brane are different from those of 3+1 dimensional general relativity. However, brane-world space-times are not the only theories that may potentially allow the existence of topologically trivial gravitational geons. One possibility, recently investigated by Dymnikova and Galaktionov, is to assume that vacuum solutions allow a varying Ricci scalar in 3+1 dimensional general relativity.

They investigated geon-like particles that they described as *vacuum non-singular*

*black holes* [38] in a spherically symmetric space-time with a de-Sitter centre. They examined a metric of the form (1.3) defined by

$$B(r) = A(r)^{-1} = 1 - \frac{2m}{r} \left( 1 - \exp\left(\frac{-r^3}{2mr_0^2}\right) \right) \quad (1.62)$$

where  $r_0^2 = \frac{3}{\Lambda}$ ,  $\Lambda$  being a cosmological constant that appears at the origin (there being no cosmological constant in the solution asymptotically). The resulting space-time is de-Sitter at its origin (i.e. having a positive cosmological constant) but Schwarzschild asymptotically (i.e. having no cosmological constant as  $r \rightarrow \infty$ ).

The authors showed that the solution has horizons for  $m$  greater than a critical value  $m_{cr}$  ( $m_{cr}$  being dependent on  $\Lambda$ ). Solutions for  $m < m_{cr}$  are static, spherically symmetric and topologically trivial gravitational geons. However, owing to the radially dependent cosmological constant,  $R \neq 0$  in general for this solution. Consequently, these solutions are not vacuum brane-world solutions of the type we are concerned with in this thesis.

Another interesting example is Vollick's 2008 paper [39] in which he looks at the possibility of stationary, asymptotically flat, non-singular and topologically trivial gravitational geons in 1+1 dimensions. He looks at two different 1+1 dimensional theories of gravity, the first being a modified Jackiw-Teitelboim theory [40, 41] of the form

$$R + \alpha R^2 + \beta \nabla_\mu \nabla^\mu R - \Lambda = 8\pi T \quad (1.63)$$

where  $\Lambda$  is a cosmological constant (in this case  $\Lambda = 0$ ). The second theory is based on the action

$$L = \sqrt{-g} \left( \frac{1}{\phi} R + V(\phi) \right). \quad (1.64)$$

In each case, working in 1+1 dimensions and treating  $r$  as a radial-like coordinate with  $r \geq 0$ , exact solutions that correspond to gravitational geons are found.

In a published addendum [42], Vollick pointed out that each of the solutions has a jump discontinuity in  $\frac{d^2 t}{d\tau^2}$  if one imposes a reflecting boundary condition at  $r = 0$  (which is necessary if there is to be a correspondence between the derived solutions and spherically symmetrical space-time solutions in 3+1 dimensions).

The author removes these discontinuities for (1.63) by allowing a non-zero cosmological constant.

In the original paper, it was shown that the field equations resulting from (1.64) would be solved by potentials of the form

$$V(\phi) = Af' \quad \text{and} \quad \frac{dV(\phi)}{d\phi} = -A^2 r^2 f''. \quad (1.65)$$

The choice of  $f(r)$  allows one to solve for the potential. In the addendum, the function

$$f(r) = 1 - \frac{2mr^2}{r^3 + 2ml^2} \quad (1.66)$$

is shown to remove the jump discontinuity and has Schwarzschild behaviour at large  $r$ .

The existence of gravitational geons similar to what we investigate herein have therefore been explored, but not previously in brane-world cosmologies.



## Chapter 2

# Gravitational Geons in Brane-World Cosmologies

In this thesis, we investigate whether the free gravitational field in the bulk modifies the gravitational field on the brane so that gravitational geons are possible on the brane. Our approach is to look at static, spherically symmetric solutions of the form

$$ds^2 = -B(r)dt^2 + A(r)dr^2 + r^2(d\theta^2 + \sin^2\theta d\phi^2). \quad (2.1)$$

The Ricci scalar for metrics of this form is

$$R = \frac{B''}{AB} - \frac{B'}{2AB} \left( \frac{A'}{A} + \frac{B'}{B} \right) + \frac{2}{Ar} \left( \frac{B'}{B} - \frac{A'}{A} \right) + \frac{2}{Ar^2} - \frac{2}{r^2}. \quad (2.2)$$

As explained in the introduction, a solution to  $R = 0$  substituted into the Einstein field equations of 3+1 dimensional general relativity, will give rise to a vacuum brane-world solution in 4+1 dimensions via a correspondence between the energy-momentum tensor in the 3+1 dimensional solution and the projection of the bulk Weyl tensor in the 4+1 dimensional solution.

Our approach is to solve  $R = 0$  in (2.2) for  $A(r)$ . We do this generally in the weak field, but for strong field results, we choose a specific function  $B(r)$ .

## 2.1 The Candidate Space-Times

We were unable to find a general solution to  $R = 0$  for (2.2). For our strong field analysis, each potential choice of  $B(r)$  represents a candidate space-time solution that may or may not correspond to gravitational geons on the brane.

We are not interested in space-time solutions with singularities so we examined the Kretschmann scalar for divergent behaviour in order to narrow down our available choices. From (1.9) and (1.10) it is clear that we must have  $\lim_{r \rightarrow 0} A(r) = 1 + O(r^n)$  with  $n \geq 2$  to avoid divergence of the Kretschmann scalar. Similarly, from (1.8) it follows that  $\lim_{r \rightarrow 0} \frac{B'(r)}{B(r)} = O(r^m)$  with  $m \geq 1$ .

In this thesis, we take

$$B(r) = 1 - \frac{2mr^2}{r^3 + 2ml^2}, \quad (2.3)$$

for which  $B'(0) = 0$ ,  $B(0) = 1$ , both  $B(r)$  and  $B'(r)$  are continuous for all  $r \geq 0$  and  $\lim_{r \rightarrow \infty} B(r) = 1 - \frac{2m}{r}$  is Schwarzschild.

In the limit as  $r \rightarrow \infty$  the gravitational field is weak and static. If we make the further assumption that any test particles are travelling at sub-relativistic speeds, we find that  $g_{tt} = -(1 + 2\Phi)$  where  $\Phi$  corresponds to the Newtonian gravitational potential. Thus knowing  $B(r)$  is sufficient for us to identify the parameter  $m$  with the gravitational mass of the space-time solution.

For (2.3) we have that  $B \approx 1 - (\frac{r}{l})^2$  for  $r \ll (ml^2)^{\frac{1}{3}}$ . Thus  $l$  has the effect of controlling the strength of a positive cosmological constant like term (with  $\Lambda = \frac{3}{l^2}$ ) that appears in the limit as  $r \rightarrow 0$  (see 3.2).

To be certain that the resulting space-times are non-singular and without horizons, we only consider solutions  $A(r)$  and  $B(r)$  greater than zero and finite for all  $r \geq 0$ .

Considering that our choice of  $B(r)$  is not unique, having chosen (2.3) and been unsuccessful at finding a general solution, we considered other candidate solutions such as those for which

$$B(r) = 1 - \frac{2mr^2}{(r+l)^3}. \quad (2.4)$$

None of the alternate expressions for  $B(r)$  that we looked at yielded a general solution to  $R = 0$  in (1.4). We decided to focus on (2.3) and use a variety of approximate and numerical methods to determine the nature of the resulting solution.

## 2.2 Methods Of Investigation

Our investigation concerns solutions to 3+1 dimensional general relativity for which the Ricci Scalar vanishes everywhere. As a consequence, (2.2) can be written as

$$A' = \frac{(2BB''r^2 - (B')^2r^2 + 4BB'r + 4B^2)A - 4B^2A^2}{Br(B'r + 4B)}. \quad (2.5)$$

We did not find a general solution to (2.5) for our choice of  $B(r)$  (2.3). In the absence of a general solution, we used a variety of analytical and numerical methods to investigate the behaviour of the candidate space-times. Using a combination of the methods described in the following sections, we were able to determine for which choices of the parameters  $m$  and  $l$  in (2.3) the solutions correspond to gravitational geons.

### 2.2.1 The Weak Field Approximation

In the absence of a cosmological constant on the brane, for  $B(r) = A(r) = 1$ , our general, spherically symmetric metric (2.1) corresponds to flat space. We therefore take the weak field limit to be  $B(r) = 1 + b(r)$  and  $A(r) = 1 + a(r)$  with  $|b(r)| \ll 1$  and  $|a(r)| \ll 1$ .

In the weak field, the differential equation that we must solve (2.5) therefore simplifies (by removing terms of second order in  $a$ ,  $a'$ ,  $b$  or  $b'$ ) to

$$a' = \frac{b''r^2 + 2b'r - 2a}{2r}. \quad (2.6)$$

With an analytical solution to this, we can determine whether there is a class of functions  $B(r)$  that correspond to gravitational geons in the weak field.

For the specific choice of  $B(r)$  that we have made (2.3), we will use our analytical solution to the weak field to verify the results that we obtain using numerical methods.

### 2.2.2 Numerical Iteration

In the absence of a general solution to (2.5), numerical methods proved very helpful in the investigation of the behaviour of the candidate space-times.

We chose to use a fourth-order Runge-Kutta method to explore (2.5) iteratively. This is expressed given an initial value problem, which in our case is

$$A' = f(r, A), \quad A(r_0) = A_0. \quad (2.7)$$

The Runge-Kutta method is then given by

$$\begin{aligned} A_{n+1} &= A_n + \frac{K_1}{6} + \frac{K_2}{3} + \frac{K_3}{3} + \frac{K_4}{6} \\ r_{n+1} &= r_n + \Delta r \end{aligned} \quad (2.8)$$

where  $\Delta r$  is the iteration length,  $A_{n+1} \approx A(r_{n+1})$  and

$$\begin{aligned} K_1 &= \Delta r f(r_n, A_n) \\ K_2 &= \Delta r f\left(r_n + \frac{\Delta r}{2}, A_n + \frac{K_1}{2}\right) \\ K_3 &= \Delta r f\left(r_n + \frac{\Delta r}{2}, A_n + \frac{K_2}{2}\right) \\ K_4 &= \Delta r f(r_n + \Delta r, A_n + K_3). \end{aligned} \quad (2.9)$$

We found that working with 3rd party software (Maple) was limiting insofar as it was slow when choosing a very small iteration length, and it proved an inflexible environment for investigating the behaviour of several variables at once. We built a custom application to address these concerns. It allowed us to choose a starting point for iteration, an iteration length, the parameters  $m$  and  $l$  as well as the range of  $r$  and the granularity for the displayed values. This produced results for certain variables of interest (see fig. 2.1). These results were then plotted using Microsoft Excel.

Knowing that there are potential singular points at  $B = 0$  and  $B'r + 4B = 0$  (2.5), using this custom application allowed us to iteratively examine the behaviour of  $A$

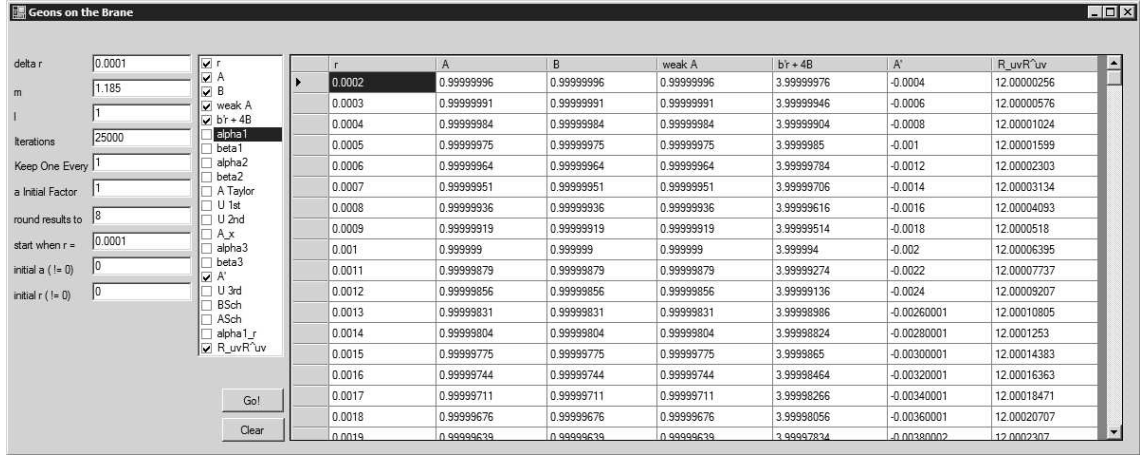


**Figure 2.1:** The interface of a custom application built to investigate our candidate space-times using a fourth-order Runge-Kutta numerical iteration.

alongside various expressions including  $B$ ,  $B'r + 4B$  and the Kretschmann Scalar ( $R_{\mu\nu\rho\sigma}R^{\mu\nu\rho\sigma}$ ) for a variety of choices of the parameters  $m$  and  $l$ . As we continued to analyse our results, we added additional expressions to the software to provide further insight into the behaviour of the solution.

It should be noted that Maple provided additional choices for methods of numerical iteration. We compared our results to those provided Maple such as the Runge-Kutta-Fehlberg adaptive numeric procedure. We found that the Maple based methods were no more successful at navigating the potential singular points in our solution. However, this comparison was invaluable for finding coding errors in our custom developed software solution as well as validating the results that we obtained.

### 2.2.3 Direction Field Plots

Numerical iteration alone was not sufficient to obtain a complete and reliable picture of the behaviour of  $A$ . In particular, we found regions of instability where the numerical solution diverged.

We used the Maple mathematics and modelling software package to produce direction field plots (for example see fig. 2.2)

Whereas the iterative approach provides results for our specific initial value

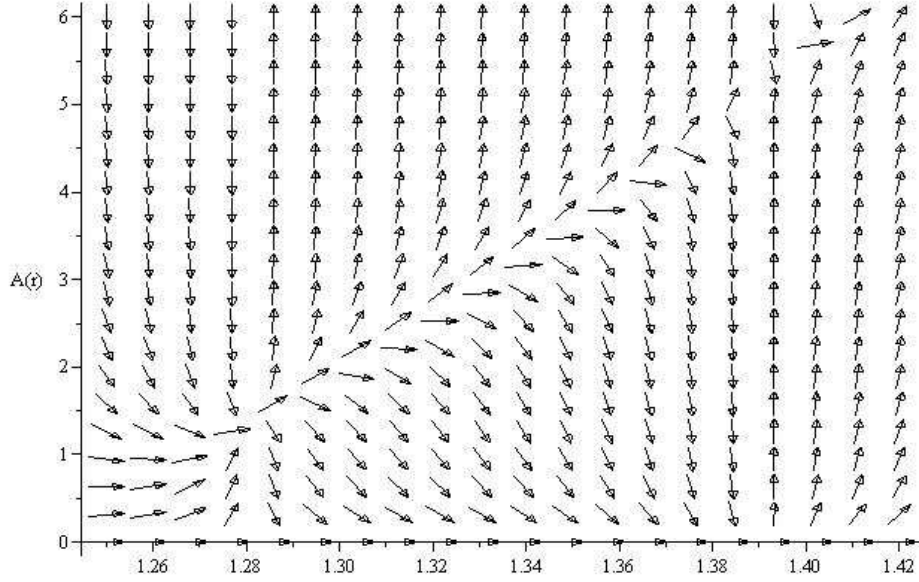


**Figure 2.2:** An example of a direction field plot showing numerical instabilities in  $A(r)$  (here plotted for  $l = 1$ ,  $m = 1.189$  and  $1.25 < r < 1.42$ ).

problem, the direction field plots indicate where there are critical points and how the behaviour of the solution depends on changes in initial conditions.

### 2.2.4 Potential Singular Points

There are potential singular points in (2.5) at  $r = 0$ ,  $B = 0$  and  $B'r + 4B = 0$ . We found solutions near these points using series approximation. Specifically, we write (2.5) in the form

$$A'(r) = f(r)A(r) + g(r)A^2(r). \quad (2.10)$$

Letting  $F'(r) = f(r)$  then (2.10) has the solution [6]

$$A(r) = \frac{-1}{e^{-F(r)} \int g(r)e^{F(r)} dr}. \quad (2.11)$$

We obtain series approximations of the form

$$\begin{aligned}
f(x) &= \sum_{n=0}^{\infty} \alpha_n x^{n+s} \\
g(x) &= \sum_{m=0}^{\infty} \beta_m x^{m+t}
\end{aligned} \tag{2.12}$$

where  $x = r - r_0$  for some potential singular point at  $r = r_0$ , the  $\alpha_n$  and  $\beta_m$  are real constants and  $s$  and  $t$  are integer constants. We can then solve (2.11) for  $\lim_{x \rightarrow 0} A(x)$ .

To ensure that the resulting space-times be non-singular and without horizons, we rule out solutions for which we find points where  $A = 0$  or  $A \rightarrow \infty$ . From the Kretschmann Scalar, (1.9) in particular, we know that solutions with  $A' \rightarrow \infty$  must also be ruled out. To that end, we differentiate our approximate solution  $A(x)$  around  $x = 0$  to obtain  $\lim_{x \rightarrow 0} A'(x)$ .

With an understanding of the behaviour of  $A$  and  $A'$  in the vicinity of a potential singular point, we can characterize the behaviour of the space-time on the spherical hypersurface corresponding to that point.

### 2.3 Weak Field Behaviour

In the weak field limit, (2.5) simplifies to (2.6) which has the solution

$$A = 1 + \frac{b'r}{2} + \frac{c}{r}, \tag{2.13}$$

where  $c$  is a constant of integration. Noting that  $c = 0$  to ensure that  $A$  be finite at  $r = 0$ , any choice of  $B(r) = 1 + b(r)$  with  $|b(r)| \ll 1$  for which  $b'r$  is small for all  $r \geq 0$  would give suitable geon solutions in the weak field.

In order to analyse candidate geons in the strong field, we have chosen  $B(r) = 1 - \frac{2mr^2}{r^3 + 2ml^2}$ . It is useful to solve this for  $A(r)$  in the weak field for which we obtain

$$A = 1 + \frac{mr^5 - 4m^2l^2r^2}{(r^3 + 2ml^2)^2}. \tag{2.14}$$

For  $r \ll (ml^2)^{\frac{1}{3}}$  we have  $B \approx 1 - (\frac{r}{l})^2$  and  $A \approx 1 - (\frac{r}{l})^2$ .  $A(r)$  therefore satisfies the requirements that  $A(0) = 1$  and that  $\lim_{r \rightarrow 0} A(r) = 1 + O(r^n)$  with  $n \geq 2$ . Furthermore,  $A(r)$  is non-zero and continuous for all  $r \geq 0$ .

It is worth noting that for large  $r$ ,  $A$  differs from Schwarzschild with  $A \approx 1 + \frac{m}{r}$ . Also, the conditions for the weak field from section (2.2.1)

$$|b(r)| = \frac{2mr^2}{r^3 + 2ml^2} \ll 1 \text{ and} \quad (2.15)$$

$$|a(r)| = \frac{mr^5 - 4m^2l^2r^2}{(r^3 + 2ml^2)^2} \ll 1 \quad (2.16)$$

are both met for  $\frac{r}{l} \ll 1$  and for  $\frac{m}{l} \ll 1$ .

For our specific choice of  $B(r)$  (see fig. 2.3), the solutions in the weak field limit correspond to gravitational geons.

We also examined the behaviour of our candidate space-times for weak fields using numerical iteration (shown in fig. 2.3 for comparison). We found that the numerical results were almost identical to the analytical results for the weak field limit.

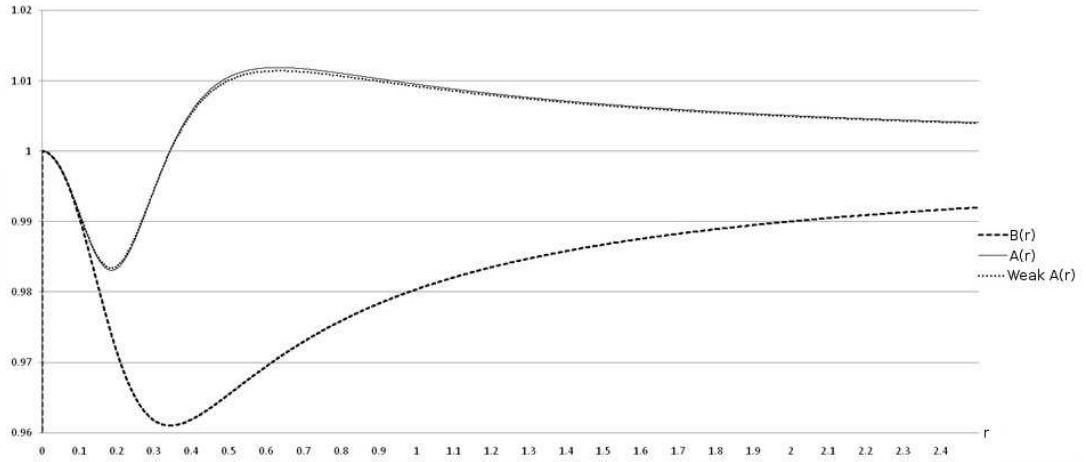


**Figure 2.3:**  $B(r)$  and  $A(r)$  plotted against radius  $r$  for  $l = 1$ ,  $m = 0.01$ . A fourth-order numerical iteration of (2.5) is labelled  $A(r)$  and the analytical weak field result is labelled *weak*  $A(r)$ . These two approaches give almost identical results for  $\frac{m}{l} \ll 1$ .



## 2.4 General Behaviour

In the absence of a general solution to (2.5) for strong gravitational fields, we examined the behaviour of  $A(r)$  using a numerical iteration. Using this method, we were unable to begin at exactly  $A(0) = 1$ . However,  $A \approx 1 - \left(\frac{r}{l}\right)^2$  for small  $r$ . Thus, if we choose an iteration length  $\Delta r$  so that  $\frac{\Delta r}{l} = 10^{-5}$  then  $A(\Delta r) \approx 1$  to within  $10^{-10}$  (independent of  $m$ ). Also, having made the observation from direction field plots that the solution is insensitive to small changes in the initial value of  $A$ , we chose  $\Delta r$  appropriately and used  $A(\Delta r) = 1$  as the starting point of the iteration.

We are interested in solutions for which both  $A(r)$  and  $B(r)$  are greater than zero and finite for all  $r \geq 0$ . The zeros of  $B$  can be determined by noting that  $B(0) = 1$ ,  $\lim_{r \rightarrow \infty} B(r) = 1$  and that  $B' = 0$  at  $r = (4ml^2)^{\frac{1}{3}}$  where  $B$  has its minimum value of  $1 - \frac{1}{3}\left(4\frac{m}{l}\right)^{\frac{2}{3}}$ . Thus

$$B \text{ has } \begin{cases} \text{no zeros} & \text{if } \frac{m}{l} < \frac{\sqrt{27}}{4} \\ \text{one zero} & \text{if } \frac{m}{l} = \frac{\sqrt{27}}{4} \\ \text{two zeros} & \text{if } \frac{m}{l} > \frac{\sqrt{27}}{4} . \end{cases} \quad (2.17)$$

We proceeded to examine the numerical iteration of  $A(r)$ . We found that it works well provided we choose  $m$  and  $l$  for which  $B'r + 4B \neq 0$  for all  $r > 0$  but that it is unable to navigate instabilities in the solution otherwise. The zeros of  $B'r + 4B$  are found by observing that  $B'r + 4B|_{r=0} = 4$ ,  $\lim_{r \rightarrow \infty} B'r + 4B = 4$  and that  $\frac{d}{dr}(B'r + 4B) = 0$  at  $r = (2ml^2)^{\frac{1}{3}}$  where  $B'r + 4B$  has its minimum value of  $4 - \left(\frac{27m}{4l}\right)^{\frac{2}{3}}$ . Thus

$$B'r + 4B \text{ has } \begin{cases} \text{no zeros} & \text{if } \frac{m}{l} < \frac{32}{27} \\ \text{one zero} & \text{if } \frac{m}{l} = \frac{32}{27} \\ \text{two zeros} & \text{if } \frac{m}{l} > \frac{32}{27} . \end{cases} \quad (2.18)$$

Noting that there will be choices of  $m$  and  $l$  for which there will be zeros of  $B'r + 4B$  but no zeros of  $B$ , we investigated the behaviour of  $A(r)$  around the zeros of  $B'r + 4B$ .

In general, from (2.10), we have

$$f(r) = \frac{2BB''r^2 - (B')^2r^2 + 4BB'r + 4B^2}{Br(B'r + 4B)} \text{ and} \quad (2.19)$$

$$g(r) = \frac{-4B}{r(B'r + 4B)}. \quad (2.20)$$

Taking  $x = r - r_0$  where  $B'r + 4B|_{r=r_0} = 0$  we get series approximations for (2.19) and (2.20)

$$f(x) = \frac{\alpha_1}{x} + \alpha_2 + \alpha_3x + O(x^2) \text{ and} \quad (2.21)$$

$$g(x) = \frac{\beta_1}{x} + \beta_2 + \beta_3x + O(x^2). \quad (2.22)$$

In this case, for  $\alpha_1 \notin \{0, -1, -2, \dots\}$ , solutions to (2.11) are of the form

$$A(x) = \frac{-1}{\frac{\beta_1}{\alpha_1} - \frac{\beta_1\alpha_2 - \beta_2\alpha_1}{\alpha_1(\alpha_1+1)}x + \lambda|x|^{-\alpha_1} + O(x^2, \lambda x|x|^{-\alpha_1})} \quad (\lambda - \text{const. of integration}). \quad (2.23)$$

For  $\alpha_1 \in \{0, -1, -2, \dots\}$  we get a different solution for each choice of  $\alpha_1$ . For example, choosing  $\alpha_1 = -1$  gives

$$A(x) = \frac{-1}{-\beta_1 + (\beta_2 + \beta_1\alpha_2)x \ln|x| + \beta_1\alpha_2x + \lambda x + O(x^2 \ln|x|)} \quad (\lambda - \text{const. of integration}). \quad (2.24)$$

However, for all choices of  $\alpha_1$  the dominant term in the denominator as  $x \rightarrow 0$  results in the same outcome that

$$\lim_{x \rightarrow 0} A(x) = \begin{cases} \frac{-\alpha_1}{\beta_1} & \text{if } \alpha_1 \leq 0 \text{ or } \lambda = 0 \\ 0 & \text{if } \alpha_1 \geq 0 \text{ and } \lambda \neq 0. \end{cases} \quad (2.25)$$

We calculated values for  $\alpha_1$  and  $\beta_1$  for each zero of  $B'r + 4B$  given a variety of values of  $m$  and  $l$  (see figs. 2.4 and 2.5).

Having verified our results for a range of choices  $0.02 < l < 750$ , we found that

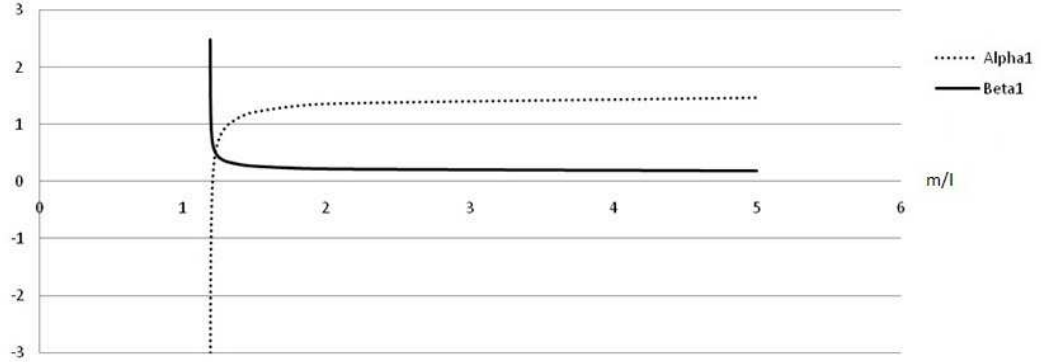


**Figure 2.4:**  $\alpha_1$  and  $\beta_1$  plotted against  $\frac{m}{l}$  for the first zero of  $B'r + 4B$ .

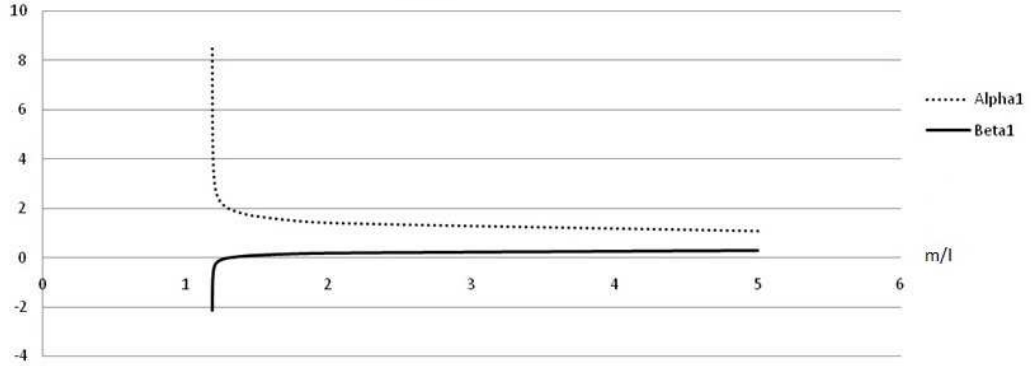


**Figure 2.5:**  $\alpha_1$  and  $\beta_1$  plotted against  $\frac{m}{l}$  for the second zero of  $B'r + 4B$ .

at each zero the values of  $\alpha_1$  and  $\beta_1$  depend on  $\frac{m}{l}$  but not on  $m$  and  $l$  individually. Knowing that zeros of  $A(r)$  correspond to singularities in the space-time, we sought to determine where  $\alpha_1 = 0$  in terms of  $\frac{m}{l}$ .

With  $x = r - r_0$ , we have  $B'r + 4B \approx x(B''r + 5B')|_{r=r_0}$  in the vicinity of each zero of  $B'r + 4B$ , so

$$\alpha_1 = \frac{2B''r - \frac{(B')^2 r}{B} + 4B' + \frac{4B}{r}}{B''r + 5B'} \Bigg|_{r=r_0}$$

$$= \left. \frac{2B''r + 7B'}{B''r + 5B'} \right|_{r=r_0}. \quad (2.26)$$

Substituting (2.26) into (2.3) for  $\alpha_1 = 0$ , we get the following quadratic in  $r^3$

$$r^6 + 14ml^2r^3 - 24m^2l^4 = 0 \quad (2.27)$$

with one positive real root corresponding to  $r \approx (1.544ml^2)^{\frac{1}{3}}$ . Substituting this into  $B'r + 4B = 0$  yields  $\frac{m}{l} \approx 1.202$ .

From (2.18), we know that there will be two zeros of  $B'r + 4B$  for  $\frac{m}{l} \approx 1.202$ . Figure 2.5 shows that  $\alpha_1 > 0$  for all  $\frac{m}{l}$  at the second zero, thus at the first zero  $\alpha_1 > 0$  when  $\frac{m}{l} > 1.202$  and  $\alpha_1 < 0$  when  $\frac{m}{l} < 1.202$ .

The preceding analysis shows how the value of  $\alpha_1$  will help us to categorize the behaviour of  $A$  around the zeros of  $B'r + 4B$  given  $\frac{m}{l}$ . As we know that  $A' \rightarrow \pm\infty$  corresponds to singular behaviour in the space-time, we perform a similar analysis of the behaviour of  $A'$ . Differentiating (2.23) gives

$$A'(x) = \frac{-\frac{\beta_1\alpha_2 - \beta_2\alpha_1}{\alpha_1(\alpha_1 + 1)} - \frac{\alpha_1\lambda|x|^{-\alpha_1}}{x} + \dots}{\left(\frac{\beta_1}{\alpha_1} - \frac{\beta_1\alpha_2 - \beta_2\alpha_1}{\alpha_1(\alpha_1 + 1)}x + \lambda|x|^{-\alpha_1} + \dots\right)^2} \quad (2.28)$$

$$\lim_{x \rightarrow 0} A'(x) = \begin{cases} \frac{\alpha_1(\beta_2\alpha_1 - \beta_1\alpha_2)}{\beta_1^2(\alpha_1 + 1)} & \text{if } \alpha_1 < -1 \text{ or } \lambda = 0 \\ -\text{sgn}(\alpha_1\lambda x) \infty & \text{if } -1 < \alpha_1 < 1 \text{ and } \lambda \neq 0 \\ 0 & \text{if } \alpha_1 > 1 \text{ and } \lambda \neq 0. \end{cases} \quad (2.29)$$

We know from (2.25) that we need not consider  $\alpha_1 \geq 0$  (unless  $\lambda = 0$ ), but the behaviour of  $A'$  does depend on whether  $\alpha_1$  is greater or less than -1 at the zeros of  $B'r + 4B$ . We therefore sought to determine where  $\alpha_1 = -1$  in terms of  $\frac{m}{l}$  and numerically found this corresponds to  $\frac{m}{l} \approx 1.191$ .

From (2.18), we know that there will be two zeros of  $B'r + 4B$  for  $\frac{m}{l} \approx 1.191$ . Figure 2.5 shows that  $\alpha_1 > -1$  for all  $\frac{m}{l}$  at the second zero, thus at the first zero  $\alpha_1 > -1$  when  $\frac{m}{l} > 1.191$  and  $\alpha_1 < -1$  when  $\frac{m}{l} < 1.191$ .

At each zero, the values of  $\alpha_1$  and  $\beta_1$  depend on  $\frac{m}{l}$  but not on  $m$  and  $l$  individually. That is not true of the values of  $\alpha_2$  and  $\beta_2$  and (2.29) tells us that we may

need  $\alpha_2$  and  $\beta_2$  in order to categorize the behaviour of  $A$  around the first zero of  $B'r + 4B$  for  $\frac{32}{27} < \frac{m}{l} < 1.191$ . However, we did determine (again verifying our results for a range of choices  $0.02 < l < 750$ ) that at each zero  $\text{sgn}(\alpha_2)$ ,  $\text{sgn}(\beta_2)$  and the ratio  $\frac{\alpha_2}{\beta_2}$  depend on  $\frac{m}{l}$  but not on  $m$  and  $l$  individually. We can therefore say that  $\text{sgn}\left(\frac{\alpha_1(\beta_2\alpha_1 - \beta_1\alpha_2)}{\beta_1^2(\alpha_1+1)}\right) = \text{sgn}\left(\frac{\alpha_1\beta_2(\alpha_1 - \beta_1\frac{\alpha_2}{\beta_2})}{\beta_1^2(\alpha_1+1)}\right)$  depends on  $\frac{m}{l}$  but not on  $m$  and  $l$  individually.

The important thing to take away from the preceding analysis is that the behaviour of  $A$  around the zeros of  $B'r + 4B$  can be effectively characterized in terms of ranges of values of  $\frac{m}{l}$ . We are not concerned with solutions for which there exist points where  $B = 0$  (i.e.  $\frac{m}{l} \geq \frac{\sqrt{27}}{4}$ ), so this leaves five ranges of values to consider with respect to the behaviour of  $A$ . Three of these correspond to solutions in which there are two zeros of  $B'r + 4B$  and are distinguished by values taken by a specific coefficient  $\alpha_1$  in the series approximation (2.21). We refer to these ranges as *low*, *medium* and *high* referring to the relative strength of the corresponding gravitational field.

- **Two Critical Points – High Range:** There are two zeros of  $B'r + 4B$  for  $1.202 < \frac{m}{l} < \frac{\sqrt{27}}{4}$ . Both zeros have  $\alpha_1 > 0$ .
- **Two Critical Points – Medium Range:** There are two zeros of  $B'r + 4B$  for  $1.191 < \frac{m}{l} < 1.202$ . The first zero has  $-1 < \alpha_1 < 0$  and the second zero has  $\alpha_1 > 0$ .
- **Two Critical Points – Low Range:** There are two zeros of  $B'r + 4B$  for  $\frac{32}{27} < \frac{m}{l} < 1.191$ . The first zero has  $\alpha_1 < -1$  and the second zero has  $\alpha_1 > 0$ .
- **No Critical Points:** There are no zeros of  $B'r + 4B$  for  $\frac{m}{l} < \frac{32}{27}$
- **The Weak Field:** See section (2.3)

With the exception of the weak field analysis (which has already been covered), we look at each of the above ranges in the following sections.

### 2.4.1 Two Critical Points – High Range

For  $1.202 < \frac{m}{l} < \frac{\sqrt{27}}{4}$ , in (2.23)  $\alpha_1 > 0$  at each zero of  $B'r + 4B$ . We therefore considered the following two situations.

**$\lambda \neq 0$  at either zero of  $B'r + 4B$ :**  $A = 0$  at either zero of  $B'r + 4B$  when  $\lambda \neq 0$ . Our analysis of the Kretschmann scalar (1.10) indicates singular behaviour of the space-time at the spherical hypersurface corresponding to either zero.

**$\lambda = 0$  at the first zero of  $B'r + 4B$ :** Noting that  $\alpha_1 > 0$  and  $\beta_1 > 0$  (see fig. 2.4), at the first zero of  $B'r + 4B$  we have  $A = \frac{-\alpha_1}{\beta_1} < 0$  (see fig. 2.6). Since  $A(0) = 1$  then  $A(r_0) = 0$  for some  $r_0 > 0$  but inside the spherical hypersurface corresponding to the first zero of  $B'r + 4B$ . Referring again to our analysis of the Kretschmann scalar, this indicates singular behaviour in the space-time at  $r_0$ . Therefore, there can be no solutions that correspond to gravitational geons for these values of  $\frac{m}{l}$ .

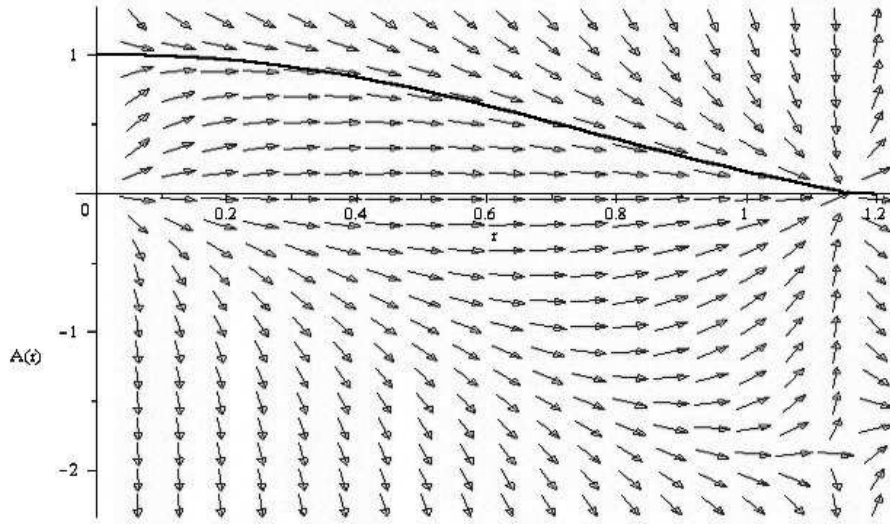


**Figure 2.6:**  $A(r)$  iteratively plotted against radius  $r$  for  $l = 1$  and  $m = 1.25$  against a direction field plot. Here, both the convergence to  $A = 0$  and  $A = \frac{-\alpha_1}{\beta_1} \approx -1.84$  at the first zero of  $B'r + 4B$  can be clearly seen.

## 2.4.2 Two Critical Points – Medium Range

For  $1.191 < \frac{m}{l} < 1.202$ , in (2.23)  $-1 < \alpha_1 < 0$  at the first zero of  $B'r + 4B$ , whereas  $\alpha_1 > 0$  at the second zero. We therefore considered the following situations.

**$\lambda \neq 0$  at the first zero of  $B'r + 4B$ :**  $A = \frac{-\alpha_1}{\beta_1}$  and  $A' \rightarrow -\text{sgn}(\alpha_1 \lambda x)^\infty$  at the zero which, from (1.9), indicates singular behaviour of the space-time.

**$\lambda \neq 0$  at the second zero of  $B'r + 4B$ :**  $A = 0$  at the second zero indicating singular behaviour in the space-time.

**$\lambda = 0$  at both zeros of  $B'r + 4B$ :** Noting that  $\alpha_1 < 0$ ,  $\beta_1 > 0$ ,  $\alpha_2 < 0$  and  $\beta_2 > 0$  at the first zero we have that  $A = \frac{-\alpha_1}{\beta_1} > 0$  and  $A' = \frac{\alpha_1(\beta_2\alpha_1 - \beta_1\alpha_2)}{\beta_1^2(\alpha_1+1)} < 0$ . At the second zero, we have  $\alpha_1 > 0$ ,  $\beta_1 < 0$ ,  $\alpha_2 < 0$  and  $\beta_2 > 0$  so that  $A = \frac{-\alpha_1}{\beta_1} > 0$  and  $A' = \frac{\alpha_1(\beta_2\alpha_1 - \beta_1\alpha_2)}{\beta_1^2(\alpha_1+1)} > 0$ . There is therefore no singular behaviour and no horizon indicated at either zero.

However, direction field plots indicate that solutions with  $A(0) = 1$  have  $A' > 0$  as the first zero of  $B'r + 4B$  is approached. Iterating backward from  $A = \frac{-\alpha_1}{\beta_1}$  at the second zero results in  $A' > 0$  as  $A$  approaches the first zero (see fig.2.7).

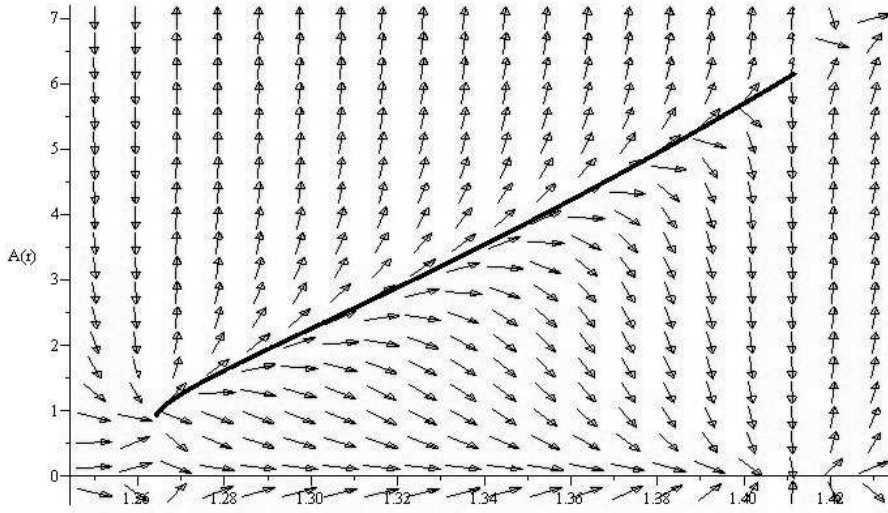


**Figure 2.7:** Reverse iteration of  $A(r)$  plotted against radius  $r$  for  $l = 1$  and  $m = 1.192$  from the second zero of  $B'r + 4B$  to the first, against a direction field plot. The solution is incompatible with the analytical result that  $A' < 0$  at the first zero for  $\lambda = 0$  solutions.

It is apparent that  $\lambda = 0$  solutions are inconsistent with our boundary conditions. We must therefore conclude that there are no solutions that correspond to gravitational geons for these values of  $\frac{m}{7}$ .

### 2.4.3 Two Critical Points – Low Range

For  $\frac{32}{27} < \frac{m}{7} < 1.191$ , in (2.23)  $\alpha_1 < -1$  at the first zero of  $B'r + 4B$ , whereas  $\alpha_1 > 0$  at the second zero. We therefore examined the behaviour of  $A$  at each zero depending on the value of the constant of integration  $\lambda$ .

**Any choice of  $\lambda$  at the first zero of  $B'r + 4B$ :**  $A = \frac{-\alpha_1}{\beta_1} > 0$  and  $A' = \frac{\alpha_1(\beta_2\alpha_1 - \beta_1\alpha_2)}{\beta_1^2(\alpha_1 + 1)} > 0$  at the first zero of  $B'r + 4B$ . There is therefore no singular behaviour and no horizon indicated.

**$\lambda \neq 0$  at the second zero of  $B'r + 4B$ :**  $A = 0$  at the second zero indicating singular behaviour in the space-time.

**$\lambda = 0$  at the second zero of  $B'r + 4B$ :**  $A = \frac{-\alpha_1}{\beta_1} > 0$  and  $A' = \frac{\alpha_1(\beta_2\alpha_1 - \beta_1\alpha_2)}{\beta_1^2(\alpha_1 + 1)} > 0$  at the second zero. No singular behaviour or horizon is indicated.

Our analysis shows the possibility of solutions corresponding to gravitational geons with  $\lambda = 0$  at the second zero, but instability at each zero prevents us from confirming any particular solution using iterative methods (see fig.2.8).

However, we have been able to confirm that  $\lim_{x \rightarrow 0} A = \frac{-\alpha_1}{\beta_1}$  and  $\lim_{x \rightarrow 0} A' = \frac{\alpha_1(\beta_2\alpha_1 - \beta_1\alpha_2)}{\beta_1^2(\alpha_1 + 1)}$  around each zero for each section constructed numerically (see figs. 2.9, 2.10 and 2.11).

We piecewise constructed  $A$  around each zero of  $B'r + 4B$  using the numerically constructed sections (see fig.2.12). The resulting solution is sewn together at the spherical hypersurfaces corresponding to each zero. The sewing together of two manifolds may induce a surface energy-momentum tensor (1.13) on the surface where they are joined.

The extrinsic curvature  $K_{\mu\nu}$  depends on the metric and its first derivatives [4]. Given that  $A$ ,  $B$  and  $B'$  are all continuous in our piecewise constructed solution, there will be a non-vanishing  $S_{\mu\nu}$  only if  $A'$  is discontinuous across either hypersurface corresponding to a zero of  $B'r + 4B$ . Our analysis shows that  $A'$  is continuous, thus implying that  $S_{\mu\nu} = 0$ .

It should be noted that there could be contributions to  $S_{\mu\nu}$  from the Weyl term



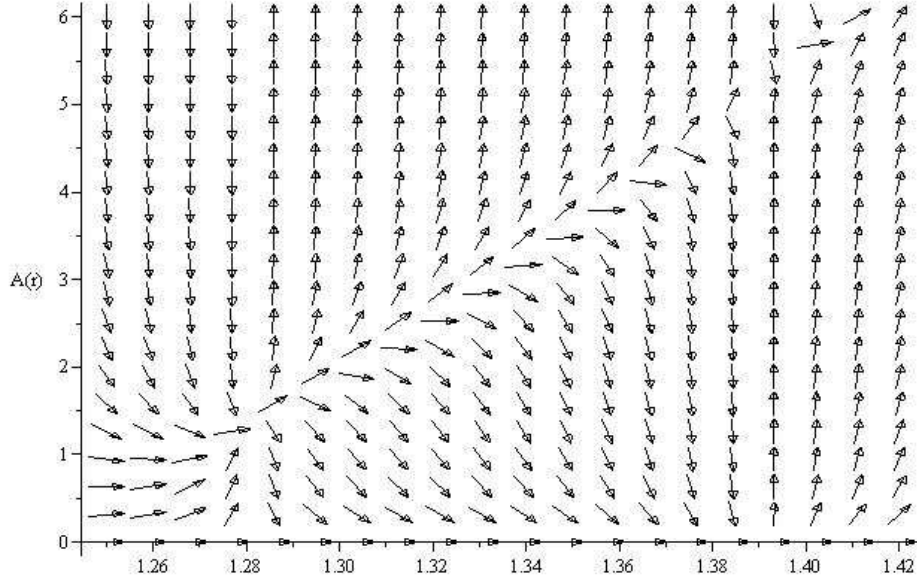


**Figure 2.8:** This direction field plot of  $A(r)$  against radius  $r$  shows that  $A(r)$  is numerically unstable at the zeros of  $B'r + 4B$ . Here we choose  $l = 1$  and  $m = 1.189$  such that the zeros are found at  $r = 1.281, 1.392$ .

(1.26). If that were the case,  $S_{\mu\nu} = 0$  in our piecewise constructed solution would imply that there is a localized gravitational source (such as matter) at the hypersurface and the stresses contributed by each cancel one another exactly. As the space-time off the brane is not known, it is not possible to check to see if such contributions exist. If there are no contributions to  $S_{\mu\nu}$  from the Weyl tensor, the piecewise constructed solutions correspond to gravitational geons.

#### 2.4.4 No Critical Points

For these values of  $\frac{m}{l}$ , all solutions with  $A(0) = 1$  correspond to gravitational geons. Choosing  $l = 1$  we confirmed the behaviour of  $A$  using iterative numerical analysis (see fig.2.13). Also evident is the progression from the weak field solution for  $\frac{m}{l} \ll 1$  (fig.2.3) to the piecewise constructed solution for  $\frac{32}{27} < \frac{m}{l} < 1.191$  (fig.2.12).

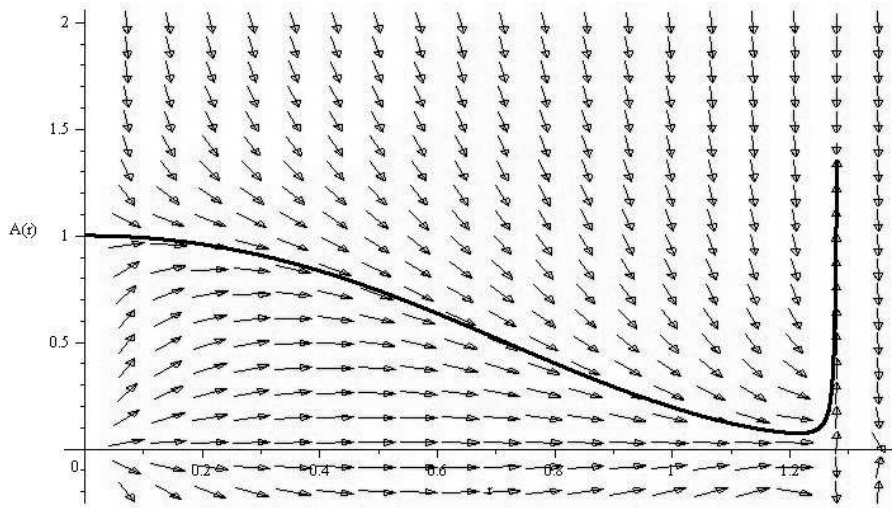


**Figure 2.9:** Forward iteration of  $A(r)$  plotted from  $r = 0$  to the first zero of  $B'r + 4B$  for  $l = 1$  and  $m = 1.189$ .  $A \rightarrow \frac{-\alpha_1}{\beta_1} \approx 1.38$  as the solution approaches the first zero.

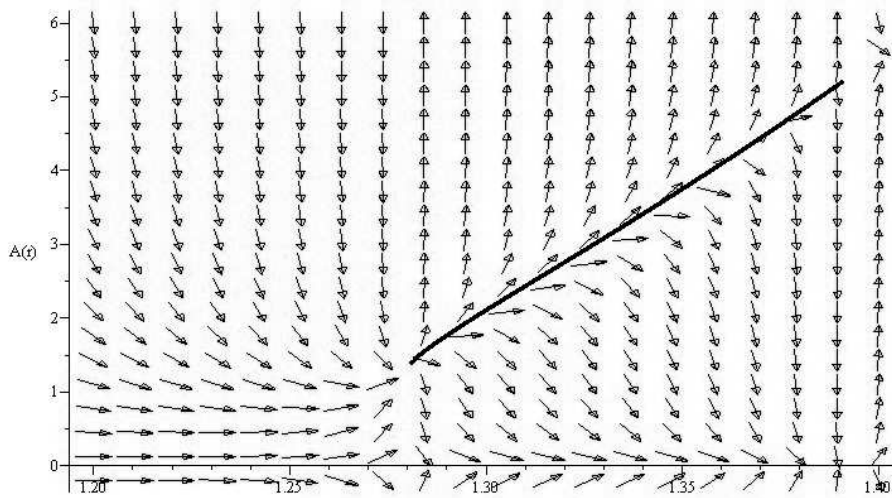


**Figure 2.10:** Reverse iteration of  $A(r)$  plotted from the second zero of  $B'r + 4B$  to the first for  $l = 1$  and  $m = 1.189$ .

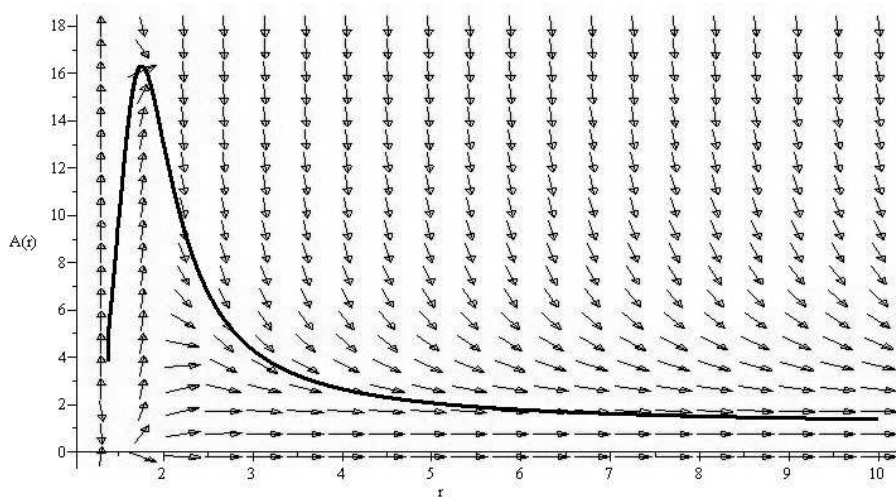


**Figure 2.11:** Forward iteration of  $A(r)$  plotted from the second zero of  $B'r + 4B$  for  $l = 1$  and  $m = 1.189$ .

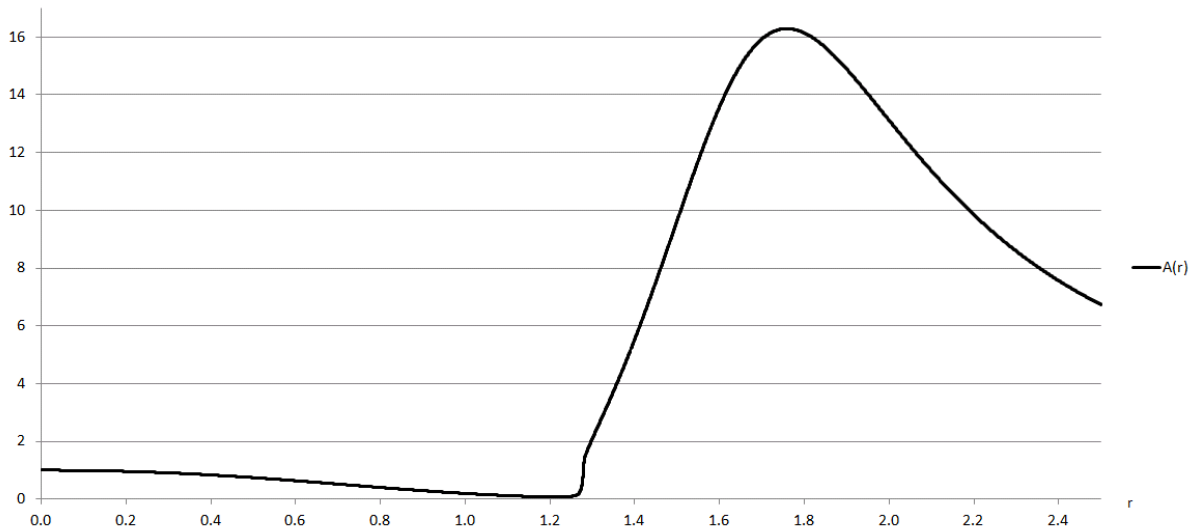


**Figure 2.12:** The function  $A(r)$  plotted against radius  $r$  for  $l = 1$  and  $m = 1.189$ . A fourth-order Runge-Kutta numerical iteration was unable to navigate the zeros of  $B'r + 4B$  (at  $r = 1.281, 1.392$ ), so the result is constructed piecewise between these points.

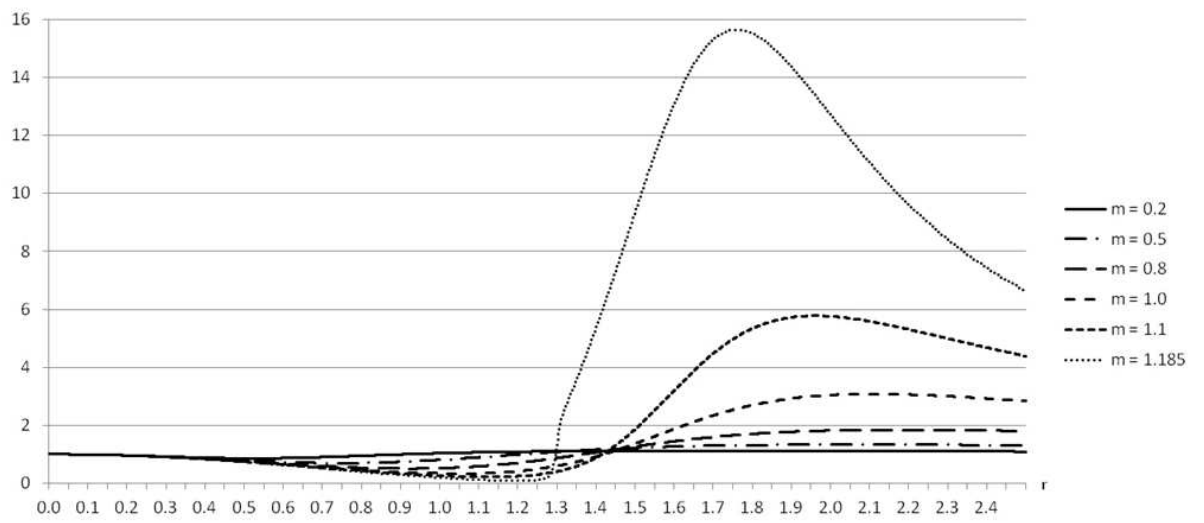


**Figure 2.13:** Function  $A(r)$  plotted against radius  $r$ . Here we choose  $l = 1$  and chart a variety of values for  $m$  in the specified region. A fourth-order Runge-Kutta numerical iteration is used to generate each result.

## Chapter 3

# Discussion And Conclusion

In this paper, we examined solutions to  $R = 0$  in 3+1 dimensional general relativity that correspond to static, spherically symmetric vacuum solutions on the brane in 5 dimensional Randall-Sundrum brane-world cosmologies. We investigated these solutions for behaviour consistent with that of gravitational geons. In the absence of a general solution, we investigated the behaviour of the space-time in the weak field approximation and used a variety of numerical and analytical methods to discover the behaviour for strong field solutions. We were able to ascertain that, for a particular range of parameter choices, gravitational geons are possible.

### 3.1 The Weak Field

In section (2.3), we found that, for metrics of the form  $B(r) = 1 + b(r)$  and  $A(r) = 1 + a(r)$  in (2.1) with weak field approximations with  $|b(r)| \ll 1$  and  $|a(r)| \ll 1$  for all  $r \geq 0$ , gravitational geons will exist as long as  $|B'r| \ll 1$  for all  $r \geq 0$ .

The main result of this thesis, that gravitational geons are possible in Randall-Sundrum brane-worlds, is achieved in the weak field, independent of the choice of  $B(r)$ . However, in order to quantitatively describe the potentially measurable presence of a gravitational geon, a specific choice of  $B(r)$  must be made.

We chose a specific  $B(r)$  and examined the corresponding space-time solution

numerically for both weak and strong fields. Our numerical analysis was largely done using a custom developed software application, the implementation of which was validated in part by the very close agreement between numerical results and analytical results for weak fields (see fig. 2.3).

Further analysis of the weak field solution could potentially show that some choices of  $B(r)$  are viable whereas others are not. This analysis would involve evolving the solution into the bulk (to be discussed in section (3.3)), and having done that, determining the stability of the solution with respect to perturbations. Without making weak field approximations, this work must be done numerically for each specifically chosen  $B(r)$ . For the analytical weak field solution, it is possible that the evolution into the bulk could be performed without resorting to numerical methods, but the degree of inaccuracy that would be introduced due to approximation is unknown.

### 3.2 Identifying $m$ and $l$

This thesis shows that in general for brane-world space-times, static, spherically symmetric and topologically trivial gravitational geons are possible. However, for the specific  $B(r)$  that we chose for our strong field analysis (2.3), gravitational geons are only viable for particular choices of the parameters  $m$  and  $l$ . The choice of  $B(r)$  is by no means unique, but it is worth looking at what these parameters represent physically as an example of how a gravitational geon solution would manifest itself as a physical entity.

$B(r)$  is Schwarzschild in the limit as  $r \rightarrow \infty$  (i.e.  $\lim_{r \rightarrow \infty} B(r) = 1 - \frac{2m}{r}$ ). In the limit as  $r \rightarrow \infty$  the gravitational field is weak and static. If we make the further assumption that any test particles are travelling at sub-relativistic speeds, we find that  $g_{tt} = -(1 + 2\Phi)$  where  $\Phi$  corresponds to the Newtonian gravitational potential. Thus knowing  $B(r)$  is sufficient for us to identify the parameter  $m$  with the gravitational mass of the space-time solution.

To get a sense of the physical significance of the parameter  $l$  it is useful to consider the metric of de Sitter space in static coordinates,

$$ds^2 = - \left(1 - \frac{\Lambda}{3} r^2\right) dt^2 + \left(1 - \frac{\Lambda}{3} r^2\right)^{-1} dr^2 + r^2(d\theta^2 + \sin^2 \theta d\phi^2), \quad (3.1)$$

where  $\Lambda$  is a cosmological constant. For our choice of  $B(r)$  we have that  $B \approx 1 - \left(\frac{r}{l}\right)^2$  for  $r \ll (ml^2)^{\frac{1}{3}}$ . Thus,  $l$  has the effect of controlling the strength of a positive cosmological constant like term (with  $\Lambda = \frac{3}{l^2}$ ) that appears in the limit as  $r \rightarrow 0$ .

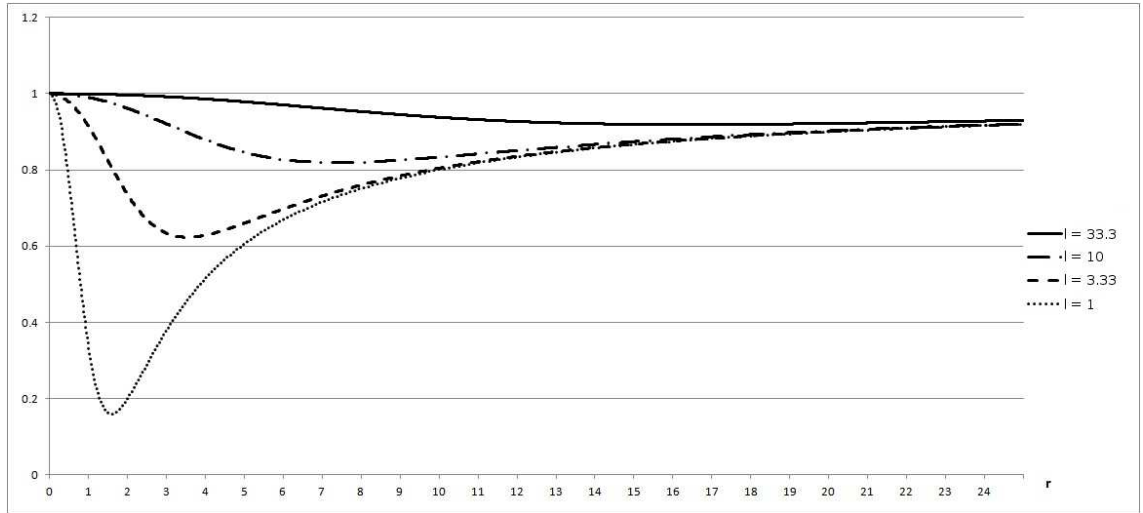


**Figure 3.1:**  $B(r)$  plotted for  $m = 1$  and  $1 \leq l \leq 33.3$ . Note that all solutions have  $\frac{m}{l} < \frac{32}{27}$  so these solutions all correspond to gravitational geons.

To see how  $l$  affects the space-time away from the radial center, see figure 3.1 in which  $B$  is shown for  $m = 1$  and varying  $l$ . For a particular choice of  $m$  there will be solutions (via appropriate choice of  $l$ ) that correspond to gravitational geons that are radially concentrated (as  $\frac{m}{l} \rightarrow \frac{32}{27}$ ) or as spread out as desired (as  $\frac{m}{l} \rightarrow 0$ ).

If we choose  $B'(r) = 0$  as a radial marker with which to assign a radial scale for our gravitational geon solutions, then observing that

$$B'(r) = \frac{2mr^4 - 8m^2l^2r}{(r^3 + 2ml^2)^2} \quad (3.2)$$

we have  $B'(r) = 0$  at

$$r = (4ml^2)^{\frac{1}{3}}. \quad (3.3)$$

We have shown that there are no solutions for the candidate space-times corresponding to gravitational geons for  $\frac{m}{l} > 1.191$ . Therefore, the lower limit on where  $B'(r) = 0$  will occur is

$$r = 1.78 \frac{Gm}{c^2}, \quad (3.4)$$

which means that in the lower limit, the radial scale of the candidate space-time solutions is of the same order as that of the Schwarzschild solution.

### 3.3 Suggestions for Further Analysis

The conclusion that static, spherically symmetric and topologically trivial gravitational geons are possible in brane-world cosmologies has been achieved in the ideal circumstance that the 3+1 dimensional space-time on the brane is an unperturbed vacuum. We have shown that such solutions (unlike the case for 3+1 dimensional general relativity) are possible. However, further analysis is necessary to determine if the candidate space-times are likely to actually occur should our universe have a Randall-Sundrum brane-world type cosmological structure.

In order to test the dynamical behaviour of our candidate space-times, a logical next analytical step would be to test for stability against small perturbations.

In this thesis, we have looked in detail at the 3+1 dimensional space-time on the brane. We are confident that solving  $R = 0$  for our candidate space-times will give rise to a vacuum brane-world solution in the 4+1 dimensional bulk [21], but the effective field equations on the brane are not a closed system. In order to test the stability of the candidate space-times, our solution must be evolved into the bulk.

The projection of the bulk Weyl tensor, which factors into the induced 3+1 dimensional field equations on the brane (1.34), is governed by a coupled system of 4+1 dimensional equations obtained from the bulk Bianchi identities [15] (round brackets around indices denote symmetrization whereas square brackets denote anti-symmetrization)



$$\begin{aligned}
\mathcal{L}_n \mathcal{E}_{AB} &= \nabla^C \mathcal{B}_{C(AB)} + \frac{1}{6} \kappa_5^2 \Lambda (K_{AB} - g_{AB} K) + K^{CD(4)} R_{CADB} \\
&\quad + 3K^C{}_{(A} \mathcal{E}_{B)C} - K \mathcal{E}_{AB} + (K_{AC} K_{DB} - K_{AB} K_{CD}) K^{CD}, \\
\mathcal{L}_n \mathcal{B}_{ABC} &= -2\nabla_{[A} \mathcal{E}_{B]C} + K_C{}^D \mathcal{B}_{ABD} - 2\mathcal{B}_{CD[A} K_{B]}{}^D, \\
\mathcal{L}_n{}^{(4)} R_{ABCD} &= -2R_{ABE[C} K_{D]}{}^E - \nabla_A \mathcal{B}_{CDB} + \nabla_A \mathcal{B}_{DCB},
\end{aligned} \tag{3.5}$$

in which  $\mathcal{E}_{AB}$  is the *electric* part of the bulk Weyl tensor (1.26) whose projection comes into the induced Einstein field equations on the brane 1.32,  $K_{AB}$  is the extrinsic curvature (1.14) ( $K = K_A{}^A$ ) and

$$\mathcal{B}_{\mu\nu\sigma} = {}^{(5)}C_{ABCD} n^D g_\mu{}^A g_\nu{}^B g_\sigma{}^C \tag{3.6}$$

is the *magnetic* part of the bulk Weyl tensor. In (3.6),  $\mathcal{B}_{\mu\nu\sigma}$  is expressed as a 3+1 dimensional tensor projected onto the brane from the 4+1 dimensional Weyl tensor, whereas in (3.5)  $\mathcal{B}_{ABC}$  is expressed as a 4+1 dimensional tensor. When evolving a solution from the brane into the bulk, the 3+1 dimensional tensors  $\mathcal{B}$  and  $\mathcal{E}$  are equated with their 4+1 dimensional counterparts by evaluating the bulk tensors on hypersurfaces in the limit approaching the brane. We therefore define boundary conditions for  $\mathcal{B}$  and  $\mathcal{E}$  at the brane in order to solve (3.5) as

$$\begin{aligned}
\nabla^A \mathcal{E}_{AB} &= \kappa_5^4 \nabla^A S_{AB}, \\
\mathcal{B}_{ABC} &= 2\nabla_{[A} K_{B]C} = \kappa_5^2 \nabla_{[A} \left( T_{B]C} - \frac{1}{3} g_{B]C} T \right).
\end{aligned} \tag{3.7}$$

We have  $R = 0$ , so for our candidate space-times, the induced field equations on the brane (1.34) become

$$\mathcal{E}_{\mu\nu} = -R_{\mu\nu}. \tag{3.8}$$

For a space-time metric of the form (2.1), the components of the Ricci tensor are [5]

$$\begin{aligned}
R_{tt} &= \frac{-B''}{2A} + \frac{B'}{4A} \left( \frac{A'}{A} + \frac{B'}{B} \right) - \frac{B'}{rA} \\
R_{rr} &= \frac{B''}{2B} - \frac{B'}{4B} \left( \frac{A'}{A} + \frac{B'}{B} \right) - \frac{A'}{rA} \\
R_{\theta\theta} &= -1 + \frac{r}{2A} \left( \frac{B'}{B} - \frac{A'}{A} \right) - \frac{1}{A} \\
R_{\phi\phi} &= R_{\theta\theta} \sin^2 \theta,
\end{aligned} \tag{3.9}$$

which for the weak field limit of our candidate space-times become

$$\begin{aligned}
R_{tt} &= \frac{-24m^2 l^2 (-r^3 + ml^2)}{(r^3 + 2ml^2)^3} \\
R_{rr} &= \frac{3m(r^6 - 18r^3 ml^2 + 8m^2 l^4)}{(r^3 + 2ml^2)^3} \\
R_{\theta\theta} &= \frac{3mr^2(-r^6 - 6r^3 ml^2 + 16m^2 l^4)}{2(r^3 + 2ml^2)^3} \\
R_{\phi\phi} &= R_{\theta\theta} \sin^2 \theta.
\end{aligned} \tag{3.10}$$

It is worth noting that, for strong fields, we would obtain these components numerically. In either case, the components of the Ricci tensor (and therefore  $\mathcal{E}$ ) are non-zero in general. When a perturbation is introduced, discovering the dynamical behaviour of  $\mathcal{E}$  (and hence the space-time both on and off the brane) depends on solving the system of equations (3.5).

The intention of performing this analysis would be to determine if there are any specific choices of the parameters  $m$  and  $l$  for which the candidate space-times are dynamically stable. Of course, in the event that none of the gravitational geon solutions that we have investigated here are stable, it is understood that the form of  $B(r)$  that we have investigated is by no means a unique choice.

Although there has been much research published regarding brane-world cosmologies in recent years, there are other modifications to the 3+1 dimensional Einstein field equations that may more accurately represent the universe in which we live. One such class of theories are known as  $f(R)$  theories (see [43] for a review). These theories are obtained when one replaces the Ricci scalar  $R$  in the Lagrangian

formulation of general relativity with a function of the Ricci scalar  $f(R)$ . The Einstein-Hilbert action

$$S_{EH} = \frac{1}{16\pi G} \int d^4x \sqrt{-g} R \quad (3.11)$$

becomes

$$S = \frac{1}{16\pi G} \int d^4x \sqrt{-g} f(R). \quad (3.12)$$

Depending on the definition of  $f(R)$ , the modified Einstein field equations may or may not admit space-time solutions corresponding to gravitational geons similar to those we have investigated here.

### 3.4 Significance of the Result

There is currently a great deal of interest in the Randall-Sundrum brane-world, which models the 3 spatial dimensions of our universe as a brane embedded in a 4+1 dimensional space-time. In 3+1 dimensional general relativity, there are no static, spherically symmetric, topologically trivial vacuum space-time solutions other than flat, empty space. In this thesis, we have shown that the same is not true for Randall-Sundrum brane world models. On the brane, there do exist static, spherically symmetric, topologically trivial vacuum space-time solutions that have mass. The source of mass for these gravitational geons derives from the bulk Weyl tensor via its contribution to the effective Einstein field equations on the brane.

Further analysis is required to show whether the candidate space-times presented here (or other candidate space-times) are likely to occur and persist in a brane-world teeming with matter and energy. Insofar as gravitational geons only interact gravitationally, they would only be observable indirectly. The possibility that gravitational geons may represent a form of dark matter has been raised before (see for example [39, 44]).

The significance of the result of this thesis is therefore that, should our universe be a Randall-Sundrum brane-world, gravitational geons represent a viable explanation for dark matter observations.

This result is also significant insofar as it adds to a body of work that shows

how space-time solutions differ between standard general relativity and Randall-Sundrum brane-worlds. It remains to be seen whether this body of work will ultimately provide evidence for or against the Randall-Sundrum brane-world model as an effective model of our universe.

# Bibliography

- [1] L. Randall and R. Sundrum, Phys. Rev. Lett. **83**, 3370 (1999) [arXiv:hep-ph/9905221]. → pages 1, 7
- [2] J. A. Wheeler, Phys. Rev. **97**, 511 (1955). → pages 1, 12
- [3] C. W. Misner, K. S. Thorne and J. A. Wheeler, *Gravitation*, (Freeman, S. Francisco, 1973), pp. 551–555 → pages 2, 3, 5
- [4] S. M. Carroll, *Spacetime and Geometry*, (Addison Wesley, S. Francisco, 2004), pp. 443–452 → pages 6, 38
- [5] S. Weinberg, *Gravitation and Cosmology: Principles and Applications of the General Theory of Relativity*, (John Wiley and Sons, Inc., 1972), pp. 172–179 → pages 2, 47
- [6] K. A. Bronnikov and S. W. Kim, Phys. Rev. D **67**, 064027 (2003) [arXiv:gr-qc/0212112]. → pages 4, 19, 28
- [7] T. Padmanabhan, *Gravitation: Foundation and Frontiers*, (Cambridge University Press, New York, 2010), pp. 552–554 → pages 5
- [8] W. Israel, Nuovo Cim. B **44S10**, 1 (1966) [Erratum-ibid. B **48**, 463 (1967)] [Nuovo Cim. B **44**, 1 (1966)]. → pages 5
- [9] T. Kaluza, Sitzungsber. Preuss. Akad. Wiss. Berlin (Math. Phys. ) **1921**, 966 (1921). → pages 6, 13
- [10] O. Klein, Z. Phys. **37**, 895 (1926) [Surveys High Energ. Phys. **5**, 241 (1986)]. → pages 6
- [11] J. M. Overduin and P. S. Wesson, Phys. Rept. **283**, 303 (1997) [arXiv:gr-qc/9805018]. → pages 6

- [12] L. Randall and R. Sundrum, Phys. Rev. Lett. **83**, 4690 (1999) [arXiv:hep-th/9906064]. → pages 7
- [13] T. Shiromizu, K. Maeda and M. Sasaki, Phys. Rev. D **62**, 024012 (2000) [arXiv:gr-qc/9910076]. → pages 7
- [14] R. Maartens and K. Koyama, arXiv:1004.3962 [hep-th]. → pages 7
- [15] M. Sasaki, T. Shiromizu and K. Maeda, Phys. Rev. D **62**, 024008 (2000) [arXiv:hep-th/9912233]. → pages 7, 46
- [16] D. Langlois, Int. J. Mod. Phys. A **17**, 2701 (2002) [arXiv:gr-qc/0205004]. → pages
- [17] R. Maartens, Frames and Gravitomagnetism, ed. J Pascual-Sanchez et al. (World Sci., 2001) pp 93-119 arXiv:gr-qc/0101059. → pages
- [18] E. Papantonopoulos, Lect. Notes Phys. **592**, 458 (2002) [arXiv:hep-th/0202044]. → pages
- [19] D. N. Vollick, Gen. Rel. Grav. **34**, 471 (2002) [arXiv:hep-th/0005033]. → pages 17
- [20] D. Wands, Class. Quant. Grav. **19**, 3403 (2002) [arXiv:hep-th/0203107]. → pages 7
- [21] N. Dadhich, R. Maartens, P. Papadopoulos and V. Rezanian, Phys. Rev. D **62**, 024008 (2000) [arXiv:hep-th/9912233]. → pages 12, 17, 46
- [22] T. Regge and J. A. Wheeler, Phys. Rev. **108**, 1063 (1957). → pages 13
- [23] A. Einstein, mass free of singularities.,” Revista Universidad Nacional de Tucuman **A2**, 11 (1941). → pages 13
- [24] A. Einstein, W. Pauli, Ann. of Math **44**, 2 (1945). → pages 13, 15
- [25] R. Serini, Rend. Lincei **27**, 235 (1918). → pages 13
- [26] A. Lichnerowicz, *Theories Relativiste de la Gravitation et de l'Electromagnetisme*, (Masson, 1955) → pages 13
- [27] J. van Dongen, Stud. Hist. Philos. Mod. Phys. **33**, 185 (2002) [arXiv:gr-qc/0009087]. → pages 13
- [28] G. D. Birkhoff, *Relativity and Modern Physics*, (Harvard University Press, Cambridge, MA, 1923) → pages 13

- [29] A. Chamblin, S. W. Hawking and H. S. Reall, *Phys. Rev. D* **61**, 065007 (2000) [arXiv:hep-th/9909205]. → pages 16
- [30] S. Shankaranarayanan and N. Dadhich, *Int. J. Mod. Phys. D* **13**, 1095 (2004) [arXiv:gr-qc/0306111]. → pages 18
- [31] E. Rodrigo, arXiv:0708.0045 [gr-qc]. → pages 19
- [32] N. Dadhich, S. Kar, S. Mukherji and M. Visser, *Phys. Rev. D* **65**, 064004 (2002) [arXiv:gr-qc/0109069]. → pages 20
- [33] D. N. Vollick, *Gen. Rel. Grav.* **34**, 1 (2002) [arXiv:hep-th/0004064]. → pages 20
- [34] D. R. Brill and J. B. Hartle, *Phys. Rev.* **135**, B271 (1964). → pages 20
- [35] F. I. Cooperstock, V. Faraoni and G. P. Perry, *Mod. Phys. Lett. A* **10**, 359 (1995). → pages 20
- [36] F. I. Cooperstock, V. Faraoni and G. P. Perry, *Int. J. Mod. Phys. D* **5**, 375 (1996) [arXiv:gr-qc/9512025]. → pages 20
- [37] R. D. Sorkin, *Topological Properties and Global Structure of Space-Time*, volume B138 of NATO Advanced Study Institutes Series, 249, edited by P.G. Bergmann and V. De Sabbata, D. Reidel Publishing Company, Dordrecht-Holland, 1986. → pages 20
- [38] I. Dymnikova and E. Galaktionov, *Class. Quant. Grav.* **22**, 2331 (2005) [arXiv:gr-qc/0409049]. → pages 21
- [39] D. N. Vollick, *Class. Quant. Grav.* **25**, 175004 (2008) [arXiv:0807.0611 [gr-qc]]. → pages 21, 49
- [40] C. Teitelboim, *Phys. Lett. B* **126** (1983) 41. → pages 21
- [41] R. Jackiw, *Nucl. Phys. B* **252**, 343 (1985). → pages 21
- [42] D. N. Vollick, *Class. Quant. Grav.* **27**, 169701 (2010) [arXiv:1004.1401 [gr-qc]]. → pages 21
- [43] T. P. Sotiriou and V. Faraoni, *Rev. Mod. Phys.* **82**, 451 (2010) [arXiv:0805.1726 [gr-qc]]. → pages 48
- [44] R. A. Sones, arXiv:gr-qc/0506011. → pages 49